IVYSPRING INTERNATIONAL PUBLISHER

Theranostics

2016; 6(11): 1899-1917. doi: 10.7150/thno.15412

Research Paper

Melatonin Treatment Improves Mesenchymal Stem Cells Therapy by Preserving Stemness during Long-term *In Vitro* Expansion

Yi Shuai[1,2*], Li Liao[1,2*], Xiaoxia Su[3], Yang Yu[1,4], Bingyi Shao[1,4], Huan Jing[1,2], Xinjing Zhang[1,4], Zhihong Deng[5✉], Yan Jin[1,2✉]

1. State Key Laboratory of Military Stomatology, Center for Tissue Engineering, School of Stomatology, Fourth Military Medical University, Xi'an, Shaanxi 710032, People's Republic of China;
2. Research and Development Center for Tissue Engineering, Fourth Military Medical University, Xi'an, Shaanxi 710032, People's Republic of China;
3. Department of Orthodontics, Stomatology Hospital of Xi'an Jiaotong University College of Medicine, Xi'an, Shaanxi 710032, People's Republic of China;
4. College of Stomatology, Chongqing Medical University, Chongqing, People's Republic of China;
5. Department of Otolaryngology, Xijing Hospital, Fourth Military Medical University, Xi'an, Shaanxi 710032, People's Republic of China.

* These authors contributed equally to the study.

✉ Corresponding authors: Yan Jin, MD. PhD. Tel: +86-29-84776147, Fax: +86-29-83218039, E-mail: yanjin@fmmu.edu.cn; Zhihong Deng, MD. PhD. Telephone: +86-29-84776472, Fax: +86-29-83218039, E-mail: dengzh@fmmu.edu.cn.

Received: 2016.03.01; Accepted: 2016.07.20; Published: 2016.08.08

Abstract

Mesenchymal stem cells (MSCs) are promising candidates for tissue regeneration and disease treatment. However, long-term in vitro passaging leads to stemness loss of MSCs, resulting in failure of MSCs therapy. Here, we report a melatonin-based strategy to improve cell therapy of in vitro cultured MSCs. Among four small molecules with anti-aging and stem cell-protection properties (rapamycin, resveratrol, quercetin and melatonin), colony forming, proliferation, and osteogenic differentiation assay showed that melatonin was the most efficient to preserve self-renewal and differentiation properties of rat bone marrow MSCs (BMMSCs) after long-term passaging. Functional assays confirmed melatonin treatment did not affect the colony forming, proliferation and osteogenic differentiation of BMMSCs cultured for 1 or 4 passages, but largely prevented the decline of self-renew and differentiation capacity of BMMSCs cultured for 15 passages in vitro. Furthermore, heterotopic osteogenesis assay, critical size calvarial defects repair assay, osteoporosis treatment and experimental colitis therapy assay strongly certified that melatonin preserved the therapeutic effect of long-term passaged BMMSCs on bone regeneration and immunotherapy in vivo. Mechanistically, melatonin functioned by activating antioxidant defense system, inhibiting the pathway of cell senescence, and preserving the expression of gene governing the stemness. Taken together, our findings showed that melatonin treatment efficiently prevented the dysfunction and therapeutic failure of BMMSCs after long-term passaging, providing a practical strategy to improve the application of BMMSCs in tissue engineering and cytotherapy.

Key words: cell culture, mesenchymal stem cells, melatonin, osteogenesis, small molecule.

Introduction

Mesenchymal stem cells (MSCs) are promising candidates for tissue regeneration and disease treatment. MSCs-based therapy is becoming increasingly popular and widely used in regenerative medicine and disease treatment [1, 2]. Until 2015, more than 500 clinical trials of MSCs therapy are approved worldwide [3]. In most cases, 10-100 million MSCs are needed for each therapy. Considering the shortage of bone marrow donation and extreme low ratio of MSCs in tissue cells, *in vitro* expansion is a

necessary procedure for MSCs application.

However, a number of disorders of MSCs have been reported to be accompanied with long-term *in vitro* passaging [4, 5]. For instance, long-term cultured MSCs display anomalous morphology and decreased expression of MSCs-specific surface antigens [6]. Long-term expansion also affects the self-renewal potency of MSCs, as shown by declined colony-forming and proliferation [6]. Furthermore, the differentiation potential of MSCs decreases after long-term passaging [5, 7]. As a result, MSCs lost the stemness necessary for tissue regeneration, leading to poor therapeutic effects. Long-term passaging decreases therapeutic effect of MSCs cytotherapy in heart diseases [8, 9], lung diseases [10], nervous system diseases [11, 12], graft versus host disease [13], lethal endotoxemia [14] and skeletal diseases [15]. It is becoming a crucial issue hindering clinical application of MSCs cytotherapy.

Physiologically, the identity and function of stem cells (SCs) are maintained by a complex network of extracellular and intracellular signaling [16]. Loss of physiological niche is the major cause of SCs dysfunction during *in vitro* passaging. Until now, a number of strategies have been applied to improve MSCs expansion by providing proper extracellular microenvironment or signaling. For instance, cultivation in hypoxic/physiologic oxygen condition [17-19] or on suitable extracellular matrix (ECM) [20, 21] , application of exogenous signaling proteins such as FGF, PDGF and EGF [22, 23], and genetic engineering [24, 25] have been applied to preserve the stemness and function of MSCs during *in vitro* expansion. However, some disadvantages of these strategies limit their application. Hypoxic or physiologic oxygen condition was reported to maintain the properties of MSCs *via* arresting cell cycle and delaying cell proliferation [26, 27]. It is difficult to ensure the source and quality of ECM in large-scale cell culture. The half-life of exogenous signaling proteins is usually short, leading to low efficiency and increased costs [28]. Genetic-modulated MSCs possess potential risk of mutation or malformation [29]. Therefore, it is urgent to find a more efficient and reliable method to obtain functional MSCs during *in vitro* expansion.

Natural small molecules are active compounds specifically and reversibly regulating signaling pathways. A number of small molecules have been reported to play profound effect on the maintenance and fate-determination of SCs [30-32]. Because of their advantages such as target-specificity, convenience of application and storage, and low cost, nature small molecules emerge as promising approaches to improve SCs therapy [33]. However, it remains challenging to preserve the function of MSCs during long-term passaging by specific small-molecule.

Melatonin, a molecule produced by pineal gland and multiple other organs [34], is an important modulator of circadian rhythms. Previous studies established that melatonin regulates various physiological functions including sleep, circadian rhythms, and neuroendocrine actions [35, 36]. Emerging evidences showed that melatonin regulates several characteristics of MSCs *in vitro* [37-40]. Melatonin treatment has been reported to promote osteogenic differentiation, vitality, and mobility of MSCs, resulting in improved MSCs therapy of skeletal defect [41], sepsis-induced kidney injury [42], acute lung ischemia–reperfusion injury [43] and skin wound healing [44]. Recently, Zhou and colleagues showed that melatonin treatment prevents H_2O_2-induced premature senescence of MSCs [45], suggesting melatonin is a promising candidate to optimize *in vitro* MSCs expansion. However, there has been no attempt to preserve the stemness of long-term passaged MSCs by melatonin treatment.

In this study, we aimed to establish a small molecule-based strategy to prevent stemness loss of BMMSCs during long-term passaging. By comparing a number of small molecules reported to preserve stem cells against senescence, we found that melatonin was the most efficient one to preserve the stemness of BMMSCs after long-term culture and improve MSCs cell therapy.

Materials and Methods

Ethics

All animal experimental procedures were approved by Animal Care Committee of the Fourth Military Medical University, Xi'an, China [SCXK (Military) 2007-007], which was in accordance with NIH Guide for the Care and Use of Laboratory Animals. The experimental procedures of human samples were approved by the Institutional Review Board for Human Subjects Research of Fourth Military Medical University (KY20163058-1). All the donors provided written informed consents for the donation of their removed bone marrows and their subsequent use in this research project.

Animals

All animals were purchased from Animal Center of Fourth Military Medical University, Xi'an, China. Seven-day-old lactational Sprague Dawley (SD) rats were used for collecting BMMSCs for *in vitro* assay or cell transplantation. Eight-week-old female NOD/SCID mice were used for ectopic bone formation assay. Eight-week-old SD female rats were used to establish calvarial defect model, OVX-induced

osteoporosis model, and experimental colitis model. All animals were housed under specific pathogen-free conditions (22°C, 12-hour light/12-hour dark cycles, and 50%–55% humidity) with free access to food pellets and tap water.

Human samples

All human samples were acquired from Department of Oral and Maxillofacial Surgery, School of Stomatology, Fourth Military Medical University. Bone marrow of ilium was derived from young donors (female, 22-25-years-old) during the operation of orthognathic surgery.

Isolation and culture of rat BMMSCs and human BMMSCs

For rat BMMSCs culture, whole bone marrow of femurs and tibias of each rat was drawn out by flushing with basal culture medium. The cell number was calculated by electronic cell counter (Bio-Rad). Total bone marrow cell number of each lactational SD rat was about 8.0×10^7, and 8.0×10^7 bone marrow cells/dish were seeded in 10-cm plastic petri dishes.

For human BMMSCs culture, bone marrow cells isolated from ilium were seeded in 10-cm plastic petri dishes containing α-MEM medium (Gibco, Grand Island, NY, USA), 10% FBS (Sijiqing, Hangzhou, China), 1% streptomycin and penicillin. BMMSCs were cultured in an atmosphere of 37℃, saturation humidity and 5% CO_2. The medium was changed every 2 days to remove the no-adherent cells, and adherent cells were cultured until they were confluent to 80%. For passaging, 0.25% trypsin/1mM EDTA (Gibco) were used to digest the cells. BMMSCs were characterized for MSCs properties before used in the following experiments.

For cell sheet culture, BMMSCs (1×10^6 cells per well) were evenly seeded in 6-well plates with 2mL basal medium per well. At confluence, the basal medium was exchanged by α-MEM containing 10% FBS and 100 mg/mL Vitamin C (Invitrogen, Carlsbad, CA, USA) for another 10-day culture. The medium was refreshed every 3 days.

Small molecule treatment strategy

Four small molecular compounds, rapamycin (molecule weight 914.17, purity ⩾ 95% (high performance liquid chromatography, HPLC), Synthetic), resveratrol (molecule weight 228.24, purity ⩾95% HPLC, Synthetic), quercetin (molecule weight 302.24, purity⩾95% HPLC, Synthetic) and melatonin (molecule weight 232.28, purity ⩾ 95% HPLC, Synthetic), were acquired from Chinese National Compound library (Shanghai, China). Each small molecule was firstly dissolved in DMSO to the concentration of 1 mM. For small molecule treatment, BMMSCs were cultured with basal medium supplemented with 10 nM small molecule since the 1st passage. BMMSCs treated with equal volume of DMSO were used as vehicle control.

Treatment of the compounds was only in the stage of cell culturing and passaging with basal medium. When the BMMSCs were cultured in osteogenic medium for differentiation or cultured to form cell sheet for transplantation, the compounds or DMSO were deprived. All cells were rinsed with PBS for 3 times to exclude the influence of residual small molecule before further analysis.

Fibroblastic Colony-forming assay

Small molecule-treated or DMSO-treated BMMSCs were digested and 5×10^2 BMMSCs were seeded in a 5-cm plastic petri dish containing α-MEM medium. The medium was refreshed every 3 days. After culturing for 10 days, the dishes were rinsed with PBS and the cells were fixed by 4% paraformaldehyde (Sigma-Aldrich, St. Louis, MO, USA). The colonies were stained by toluidine blue solution (0.1g toluidine blue powder was completely dissolved in 10 mL tri-distilled water to prepare 1% (w/v) working solution) (Sigma-Aldrich). Cell aggregate containing more than 50 cells under the stereomicroscope (Olympus Optical, Tokyo, Japan) was identified as a colony. The colony ratio was calculated as colony numbers/500 (%) [46].

Cell proliferation assay

BMMSCs (1×10^3 cells/well) were seeded in 96-well plates. Cell proliferation was analyzed with a cell counting kit-8 (CCK-8, Dojindo, Kumamoto, Japan) following the standard protocol. In brief, 10 μL CCK-8 solution per 100 μL medium was added into intraday wells, and the plates were incubated in an atmosphere of 37℃, saturation humidity and 5% CO_2 for 2 hr after being blended. The OD value was recorded by a microplate reader (Bio-TEK Instruments, Winooski, VT, USA) at 450 nm. The assays were performed from day 0 to day 6. The OD values of the following days were normalized to the values of day 0.

Osteogenic differentiation assay

For osteogenic differentiation assay, 1×10^5/well BMMSCs were seeded in 12-well plates. Osteogenic medium containing 5 mM β-glycerophosphate (Sigma-Aldrich), 50 μg/mL ascorbic acid (Sigma-Aldrich) and 10 nM dexamethasone (Sigma-Aldrich) was added to plates after the cells reached 80% confluence. Osteogenic medium was refreshed every 3 days.

For ALP staining, BMMSCs were rinsed with

PBS and fixed by 4% paraformaldehyde 7 days after induction. ALP staining was performed with a commercial kit (Beyotime, Shanghai, China) according to the protocol. Photos were taken and the staining was quantified with Image-Pro Plus 6.0 (Media Cybernetics, Rockville, MD, USA). B-ALP activity of BMMSCs was analyzed using a commercial ELISA kit (Yanhui, Shanghai, China) according to the protocol. The values were normalized to corresponding total protein concentrations. For alizarin red staining, cells were cultured with osteogenic medium for 28 days. Alizarin red (Sigma-Aldrich) staining was performed according to the instruction. For quantification, the stained mineralized nodules were dissolved with 6% cetyl-pyridine, and the OD value was tested by a microplate reader (Bio-TEK Instruments) at 570 nm.

RNA extraction and real-time RT-PCR of mRNA

Total RNA was extracted by Trizol reagent (Invitrogen, USA) according to the protocol. 1000 ng total RNA was reverse transcribed to cDNA using a PrimeScript RT reagent kit (TaKaRa, Japan). Real-time RT-PCR analysis was performed using the SYBR Premix Ex Taq II kit (TaKaRa) and tested by a CFX96TM Real-time RT-PCR System (Bio-Rad, Hercules, CA, USA). *β-actin* was used as the internal control for quantitation of target mRNA. The primer sequences for real-time RT-PCR were given in Supplementary Table S1.

Experiment design of ectopic bone formation assay

P1, P4, P15 BMMSCs treated with DMSO and P15 BMMSCs treated with melatonin were cultured to form cell sheets as described above. Four layers of BMMSCs sheets were composited with three layers of HA/TCP (20 mg in total, HA to TCP=6:4, particles 50-200 nm) to create a sandwich structure and then were packaged as a block mass for subcutaneous transplantation. Sixteen 8-week-old NOD/SCID mice were randomly divided into four groups (P1, P4, P15 and P15+mel). Under general anesthesia (30 mg/kg pentobarbital sodium), the implants composed of cell sheets and HA/TCP were transplanted subcutaneously on the back of nude mice. 8 weeks after implantation, NOD/SCID mice sacrificed and the implants were obtained for histological assay. The implants were fixed by 4% paraformaldehyde for 48 hr and decalcified with 17% EDTA (Gibco) for 2 weeks. After being embedded with paraffin, samples were sliced and stained with hematoxylin and eosin (H&E) (Sigma-Aldrich) or Masson's trichrome (Sigma-Aldrich). The bone formation regions were photographed under a light and polarized microscopy (Olympus Optical) and were evaluated by Image-Pro Plus 6.0 (Media Cybernetics) from 3 randomly selected views of each specimen.

Experiment design of critical size calvarial defects repair assay

Sixteen 8-week-old SD rats were randomly and equally distributed into four groups (P1, P4, P15 and P15+mel). Under general anesthesia, parts of bone at the central of calvarium were removed to form a roundness critical defect of 8 mm in diameter (thickness of the skull≈0.5 mm, volume≈25.13 mm^3). Four layers of BMMSCs sheets were composited with three layers of HA/TCP (50 mg in total) to create a sandwich structure for calvarial defect repair. BMMSCs treated with melatonin from the 1^{st} to the 15^{th} passage was used in P15+mel group. BMMSCs treated with equal volume of DMSO (as vehicle control) for 1, 4, and 15 passages were used in P1, P4 and P15 group. All rats were sacrificed 12 weeks after transplantation and the skulls were fixed in 4% paraformaldehyde.

Reparative effect of BMMSCs was analyzed by micro-CT (Siemens Inveon, Eschborn, Germany) in terms of the scanning protocol (voltage of 80 kV, current of 500 mA and isotropic resolution of 14.97 mm). New bone formation was analyzed using Inveon Research Workplace 2.2 (Siemens). After micro-CT scanning, all skulls were decalcified by 17% EDTA, embedded with paraffin and sliced in the coronal plane for hematoxylin and eosin (H&E) staining. The regenerative junctions were photographed under a light and polarized microscopy (Olympus).

Experiment design of osteoporosis treatment by systemic injection of BMMSCs

Thirty-six 8-week-old SD rats were randomly and evenly divided into 6 groups (Sham, OVX, OVX+P1, OVX+P4, OVX+P15 and OVX+P15+mel). Under general anesthesia, rats in Sham group were only resected some fat near ovaries and rats in the rest groups were resected bilateral ovaries. Twenty-four hours after operation, DMSO-treated P1, P4, P15 BMMSCs and melatonin-treated P15 BMMSCs were injected respectively *via* tail vein at the concentration of 2×10^7 cells/kg. Rats in Sham and OVX group were administrated with equal volume of PBS. To label new bone formation, calcein (8 mg/kg, Sigma-Aldrich) was subcutaneously injected into all rats 10 days and 3 days before sacrifice. Ten weeks after surgery, both femurs were isolated after sacrifice and fixed in 4% paraformaldehyde. The left femurs were used for three-point bending test, while the distal parts of left

femurs were used for hard tissue slicing to detect calcein labeling.

The right femurs were analyzed by micro-CT (GE, Fairfield, CT, USA) according to the scanning protocol (voltage of 80 kV, current of 80 μA and isotropic resolution of 14 mm). Bone mass density (BMD) and trabecular bone parameters were calculated with self-contained software system (GE). After micro-CT analysis, Femurs were then decalcified, embedded and sliced for H&E staining and tartrate-resistant acid phosphatase (TRAP) staining (Sigma-Aldrich) according to the standard protocol.

Three-point bending assay

For mechanical analysis of femurs of osteoporosis models, the left femurs were subjected to a vertical loading by a wedge-shaped punch in terms of constant parameters (span: 25 mm, speed: 0.5 mm/min) in a loading machine (AGS-10kNG, 500N) (Shimadzu, Kyoto, Japan). When the femur was fractured, bending resistance was evaluated according to the formula: $S_f=1.5\times F\times L/(b\times d^2)$. ($S_f$: bending strength (Mpa), F: maximum load (N), L: span (mm), b: sample width (mm), d: sample thickness (mm)).

Calcein labeling assay

OVX-induced osteoporosis rats were subcutaneously injected with calcein (8 mg/kg, Sigma) at 3 days and 10 days before sacrifice. The distal parts of left femurs were resected, fixed with 4% paraformaldehyde, and embedded in polymethyl acrylate. The specimens were cut into 50 μm thick sections and the calcein labeling was detected under a fluorescence microscope (Olympus). The distance between 2 layers of calcein was measured with Image Pro software to evaluate bone-formation rate.

Experiment design of experimental colitis treatment by systemic injection of BMMSCs

For injection of rat BMMSCs, twenty-four 8-week-old SD rats were randomly and evenly divided into 6 groups (normal, DSS, DSS+P1, DSS+P4, DSS+P15 and DSS+P15+mel). Rats of DSS, DSS+P1, DSS+P4, DSS+P15 and DSS+P15+mel group were fed with 3% (w/v) dextran sulfate sodium (DSS, Millipore, Billerica, MA, USA) in water for 10 days. Rats of normal group were fed with purified water only. At day 3, rats of DSS+P1, DSS+P4, DSS+P15 and DSS+P15+mel group were intravenously administrated with P1, P4, P15 and melatonin-treated P15 BMMSCs (1×10^7 cells/kg), respectively. Rats in normal and DSS group were administrated with equal volume of PBS. The mortality and body weight were recorded every day. Disease activity index (DAI) calculated according to changes of body weight, diarrhea and hematochezia as previously described [47]. Seven days after BMMSCs injection, colons were entirely resected for length measurement and pathological analysis. For pathological analysis, the colon segments were fixed with 4% paraformaldehyde, embedded in paraffin, cut into 4 μm-thick sections and subjected to H&E staining. The conditions of inflammation and edema of colons were evaluated under a light and polarized microscopy. The pathological index was assessed as previously reported [48]. For injection of human BMMSCs, twenty-four 8-week-old SD rats were randomly and evenly divided into 6 groups (normal, DSS, DSS+P1, DSS+P4, DSS+P25 and DSS+P25+mel). All the procedures were performed as mentioned above.

Oxidative stress analysis

Intracellular reactive oxygen species (ROS) levels were detected using a Reactive Oxygen Species Assay Kit (Beyotime). Briefly, cells were digested, rinsed and resuspended in serum-free medium, and labeled with 25 mM 2', 7'-dichlorofluorescein diacetate (DCFH-DA). The cell suspension was incubated in 37℃ for 30 min and blended every 5 min. Afterwards, cells were rinsed, collected and suspended in PBS and detected at 488 nm excitation and 525 nm emission wavelength by flow cytometer (Beckman Coulter, Fullerton, CA, USA).

Western blot analysis

The samples used for western blot assay were total protein isolated from *in-vitro* cultured P1, P4, P15 BMMSCs treated with DMSO and P15 BMMSCs treated with melatonin or melatonin+luzindole. Exogenous P1, P4, P15, P15+mel and P15+mel+LUZ BMMSCs were rinsed and collected. Cells were lysed both by cell lysis buffer supplemented with protease inhibitors and ultrasonic at low frequency. The precipitates were discarded after centrifugation and the supernatant containing total proteins were collected for western blot analysis. Equal amounts of proteins were loaded on 15% SDS-PAGE. After separation, proteins were transferred to polyvinylidene fluoride membranes (Millipore). The membranes were blocked with 5% nonfat milk powder blocking buffer and then were incubated overnight (at least 8 hr) at 4℃ with the primary antibody for rat SOD2 (Cell Signaling Technology, USA), NANOG (Cell Signaling), p53 (Santa Cruz Biotechnology, USA), p16 (Abbiotec. LLC, USA), Mel-1A-R (Santa Cruz Biotechnology), Mel-1B-R (Abcam) respectively. The membranes were then incubated with secondary antibody (Boster, China) at room temperature for 2 hr after rinsing. The blots on

the membranes were developed in a protein enhancement imaging system under treatment of an enhanced chemiluminescence kit (Amersham Biosciences, USA). The gray values of the blots were analyzed by Photoshop CS7 (Adobe Systems, USA). The value of each blot was normalized to the value of β-actin.

Immunofluorescence staining

Immunofluorescence staining was performed as described previously [49]. Cells were fixed, rinsed and treated with 0.2% Triton X-100 (Sigma-Aldrich). After rinsing, cells were incubated overnight (at least 8 hr) at 4 ℃ with the primary antibody for rat SOD2 (Cell Signaling), NANOG (Cell Signaling), p53 (Santa Cruz Biotechnology), p16 (Abbiotec) respectively. After rinsing, cells were incubated with fluorescent secondary antibody (Cell Signaling) at room temperature for 2 hr. The cell nuclei were counterstained by Hoechst 33342 (Sigma-Aldrich) for 10 min at room temperature. The results were examined under a confocal microscope (Olympus). The original and merged images were captured and performed by DP controller or DP manager (Olympus).

Inhibition of melatonin receptors

To inhibit the signaling mediated by melatonin receptors, 1000 nM Luzindole (molecule weight 292.38, purity≥96% HPLC, Synthetic) (Abcam, USA), a non-selective antagonist of melatonin receptors, was added in the basal medium 30 min before supplement with melatonin during passaging.

Statistical analysis

All the data were displayed as mean±S.D. Comparisons were performed by Student's t-test or one-way ANOVA using SPSS 13.0 (SPSS Inc, USA). Significance was confirmed at $p<0.05$. Specific p values were added in figures.

Results

The Stemness of rat BMMSCs is decreased after long-term passaging.

To determine the effect of long-term *in vitro* passaging on the stemness of BMMSCs, we chose rat BMMSCs cultured for 1 passage (P1), 4 passages (P4) and 15 passages (P15) for analysis. Colony forming assay showed that P1 and P4 BMMSCs formed similar numbers of fibroblastic colony forming unit (CFU-F) (n=3, $p>0.05$) (Fig. 1A). Proliferation assay showed that the growth rate of P1 BMMSCs was similar to that of P4 BMMSCs (n=3, $p>0.05$) (Fig. 1B). ALP staining and bone-ALP (B-ALP) ELISA showed that activity of ALP and B-ALP, enzymes indispensable for mineralization, was comparable between P1 and P4 BMMSCs (n=3, $p>0.05$) (Fig. 1C). Alizarin red staining revealed that mineralized nodules formed by P4 BMMSCs were slightly less than P1 BMMSCs (n=3, $p<0.05$) (Fig. 1D). Furthermore, real-time RT-PCR analysis showed that the expressions of *Runx2* and *Ocn*, two markers of osteogenesis, were only decreased by ~20% at passage 4 (n=3, $p<0.05$) (Fig. 1E). However, we found that colony formation ratio of P15 BMMSCs was decreased by 64% (n=3, $p<0.001$), while their proliferation capacity was significantly decreased (n=3, $p<0.01$), compared with P1 BMMSCs (Fig. 1, A and B). ALP and B-ALP activity of P15 BMMSCs was respectively reduced to 57% or 46% of that of P1 BMMSCs (n=3, $p<0.001$) (Fig. 1C), and mineralized nodules formed by P15 BMMSCs was reduced to 32% of P1 BMMSCs (n=3, $p<0.001$) (Fig. 1D). *Runx2* and *Ocn* mRNA levels were decreased by more than 50% in P15 BMMSCs (n=3, $p<0.001$) (Fig. 1E). Taken together, these data indicate that the stemness of BMMSCs is significantly decreased after long-term passaging.

Melatonin preserves the stemness of BMMSCs during long-term passaging.

To explore a small molecule-based strategy to prevent the loss of stemness of BMMSCs during passaging, we selected rapamycin, resveratrol, quercetin and melatonin, four compounds generally acknowledged as anti-aging or stem cell-protection substances, as candidates. Each small molecule was separately supplemented to basal medium during BMMSCs culture from the 1st passage to the 15th passages.

CFU assay exhibited that resveratrol, quercetin and melatonin all improved colony formation of P15 BMMSCs (n=3, $p<0.001$) (Fig. 2A), while rapamycin inhibited the colony forming ability of P15 BMMSCs (n=3, $p<0.05$), compared with DMSO-treated (as vehicle control) P15 BMMSCs (Fig. 2A). Notably, melatonin increased colony formation ratio of P15 BMMSCs by 2.5 times (n=3, $p<0.001$), which was the most significant among these small molecules (Fig. 2A). Proliferation assay revealed that rapamycin inhibited cell growth (n=3, $p<0.01$) (Fig. 2B), while resveratrol did not affect the proliferation of P15 BMMSCs (n=3, $p>0.05$) (Fig. 2B). Only quercetin and melatonin (n=3, $p<0.001$) significantly promoted the proliferation of P15 BMMSCs (Fig. 2B). It is notable that melatonin performed better promotion effect than quercetin since day 5 (n=3, $p<0.05$) (Fig. 2B). Alizarin red staining and real-time RT-PCR assay showed that rapamycin slightly inhibited osteogenic differentiation of P15 BMMSCs (n=3, $p<0.05$) (Fig. 2, C to E). Resveratrol and quercetin slightly elevated

osteogenic differentiation capacity of P15 BMMSCs (n=3, $p<0.05$ or $p<0.001$) (Fig. 2, C to E). Only melatonin treatment led to a 3-fold or 2-fold increase of ALP or B-ALP activity (n=3, $p<0.001$) and mineralized modules formation (n-3, $p<0.001$), and a 2-fold increase of *Runx2* (n=3, $p<0.001$) and *Ocn* (n=3, $p<0.001$) mRNA levels, compared with DMSO-treated P15 BMMSCs (Fig. 2, C to E). Taken together, melatonin was the most efficient one to maintain the stemness of long-term passaged BMMSCs among 4 small molecules.

We performed an experiment to screen an optimal concentration of melatonin from a range of dosages (0 nM, 1 nM, 10 nM, 100 nM, 1000 nM). According to the results, melatonin of 1 nM, 10 nM or 100 nM efficiently preserved the self-renewal and osteogenic potential of P15 BMMSCs (n=3, $p<0.05$) (Fig. S1), whereas melatonin of 1000 nM disturbed the colony forming and differentiation of P15 BMMSCs (n=3, $p<0.05$) (Fig. S1). Moreover, effects of melatonin at 10 nM and 100 nM were comparable (n=3, $p>0.05$), and were better than other concentrations on stemness preservation of long-term passaged BMMSCs (n=3, $p<0.05$) (Fig. S1). Although 100 nM showed no toxicity to BMMSCs in our study, we preferred to choose 10 nM in further study than 100 nM in consideration of biosecurity and economy.

To investigate whether melatonin functions by preventing the stemness loss after long-term passaging or by directly promoting the stemness of BMMSCs, we analyzed the function of melatonin-treated BMMSCs at P1, P4, and P15 respectively. Colony formation (n=3, $p<0.001$), proliferation (n=3, $p<0.01$) and osteogenesis analysis (n=3, $p<0.01$) confirmed that melatonin largely recovered the self-renewal and osteogenic differentiation properties of P15 BMMSCs (Fig. 3, A to E). However, melatonin did not affect the function of P1 and P4 BMMSCs (n=3, $p>0.05$) (Fig. 3, A to E), suggesting melatonin functions majorly by preventing the stemness loss during long-term passaging.

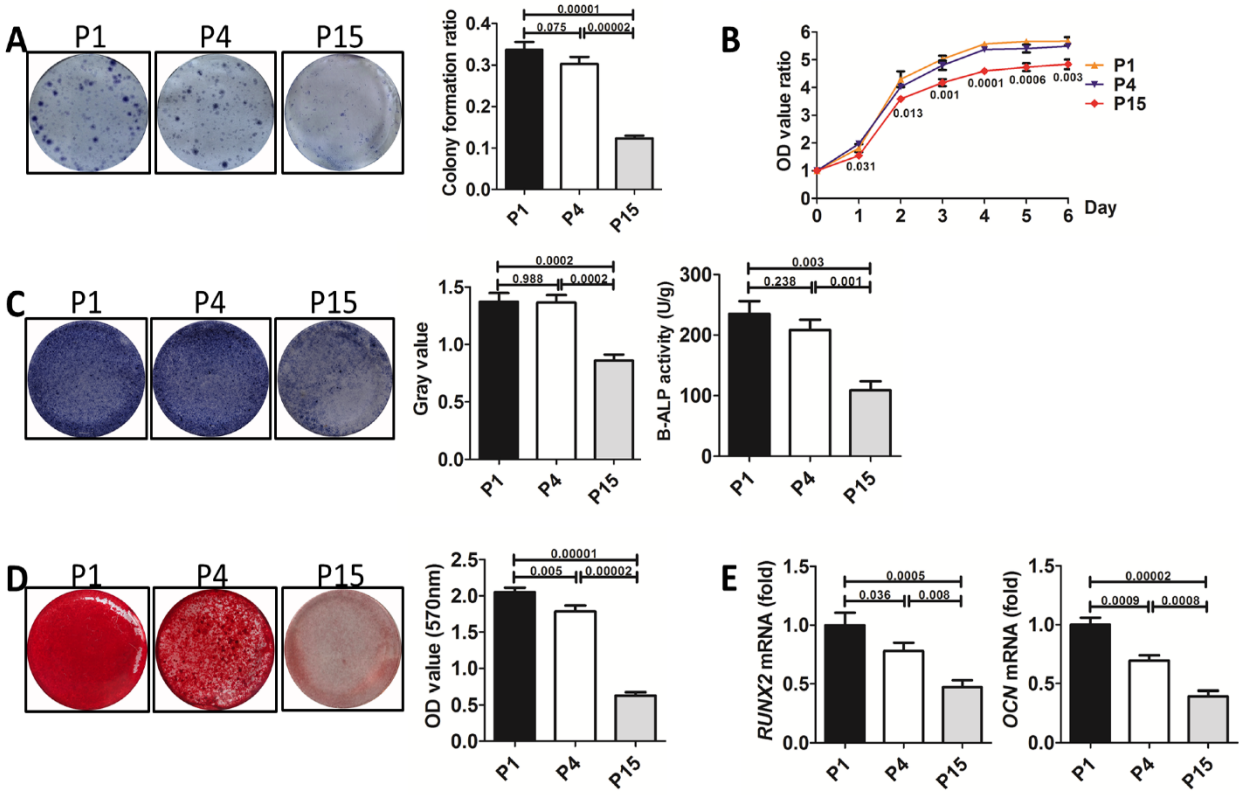

Figure 1. Self-renewal and osteogenic differentiation capacities of BMMSCs are decreased after long-term passaging. Rat BMMSCs cultured for 1 passage (P1), 4 passages (P4), and 15 passages (P15) were used in the following analysis. (**A**) 5×10^2 BMMSCs were seeded in 5-cm dishes for 10 days. CFU-F was analyzed by toluidine blue staining and the colony ratio was counted (n=3). (**B**) 1×10^3/well BMMSCs were seeded in 96-well plates. Proliferation of BMMSCs was detected from day 0 to day 6 (n=3). (**C**) 1×10^5/well BMMSCs seeded in 12-well plates were induced with osteogenic medium for 7 days. Activity of ALP was detected by ALP staining and quantified with Image-Pro Plus 6.0 software (n=3). Activity of B-ALP was detected by ELISA and values were normalized to corresponding total protein concentration (n=3). (**D**) BMMSCs were induced with osteogenic medium for 28 days. Mineralized nodules were detected by alizarin red staining and quantified with a spectrophotometer after dissolving with isopropanol (n=3). (**E**) *Runx2* and *Ocn* mRNA levels of BMMSCs were analyzed by Real-time RT-PCR. *β-actin* was used as the loading control for quantification (n=3). Data are shown as mean±SD. *P* value is presented in each graph.

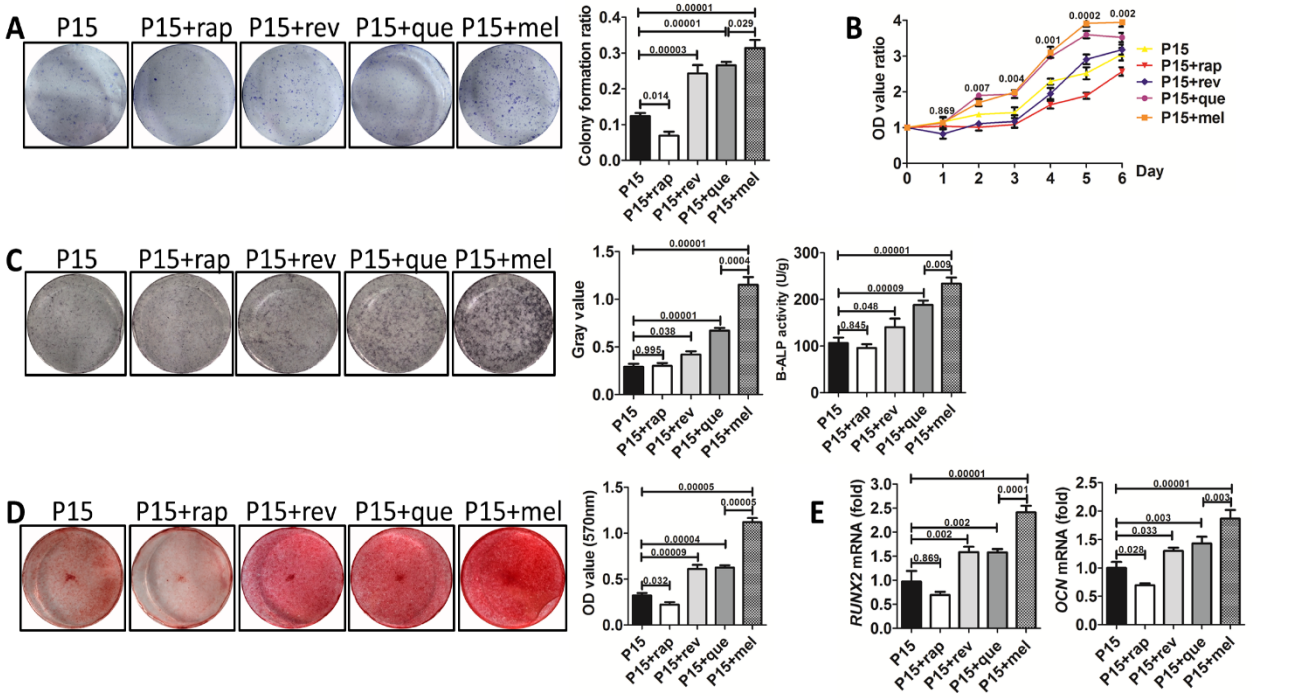

Figure 2. The effect of four small molecules on the stemness of long-term passaged BMMSCs. P15 rat BMMSCs were treated with 10 nM rapamycin, resveratrol, quercetin, melatonin or equal volume of DMSO (vehicle control) separately from the 1st passage to the 15th passage before analysis. (**A**) CFU-F formation of P15 BMMSCs was detected by toluidine blue staining and calculated (n=3). (**B**) Proliferation of P15 BMMSCs was detected from day 0 to day 6 (n=3). (**C**) ALP activity of P15 BMMSCs was tested after 7-day osteogenic induction and quantified with Image-Pro Plus 6.0 software (n=3). Activity of B-ALP was detected by ELISA and values were normalized to corresponding total protein concentration (n=3). (**D**) Mineralized nodules formed by P15 BMMSCs were tested by alizarin red staining after 28-day osteogenic induction and quantified with a spectrophotometer (n=3). (**E**) *Runx2* and *Ocn* mRNA levels of P15 BMMSCs were analyzed by Real-time RT-PCR. *β-actin* was used as the loading control for quantification (n=3). Data are shown as mean±SD. *P* value is presented in each graph.

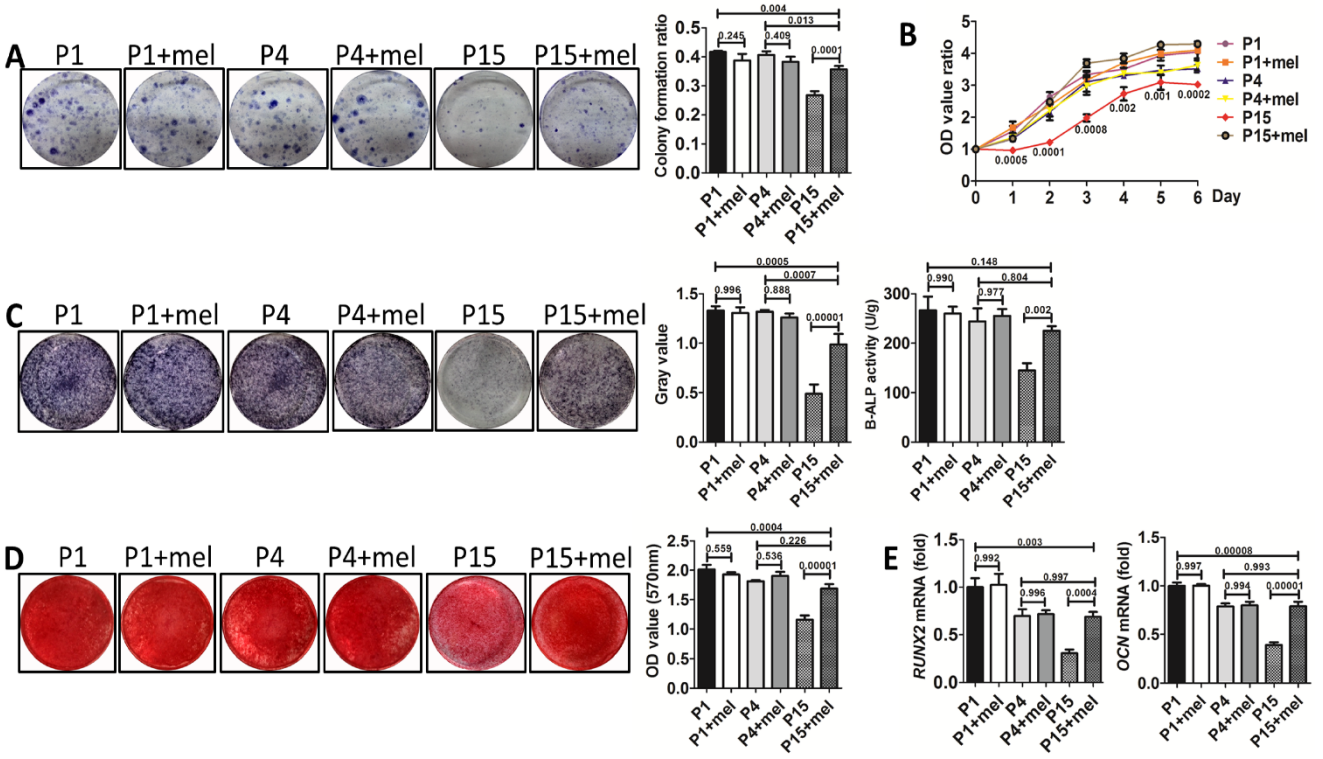

Figure 3. Melatonin prevents the stemness loss of long-term passaged BMMSCs. Rat BMMSCs of melatonin treatment group were treated with melatonin from the very beginning of the 1st passage to the 1st (P1+mel), 4th (P4+mel), or 15th passage (P15+mel). BMMSCs treated with DMSO for 1, 4 or 15 passages were used as vehicle control. (**A**) CFU-F of BMMSCs was analyzed by toluidine blue staining and calculated (n=3). (**B**) Proliferation of BMMSCs was detected from day 0 to day 6 (n=3). (**C**) ALP activity of BMMSCs was tested after 7-day osteogenic induction and quantified with Image-Pro Plus 6.0 software (n=3). Activity of B-ALP was detected by ELISA and values were normalized to corresponding total protein concentration (n=3). (**D**) Mineralized nodules formed by BMMSCs were tested by alizarin red staining after 28-day osteogenic induction and quantified with a spectrophotometer (n=3). (**E**) *Runx2* and *Ocn* mRNA levels of BMMSCs were analyzed by Real-time RT-PCR. *β-actin* was used as the loading control for quantification (n=3). Data are shown as mean±SD. *P* value is presented in each graph.

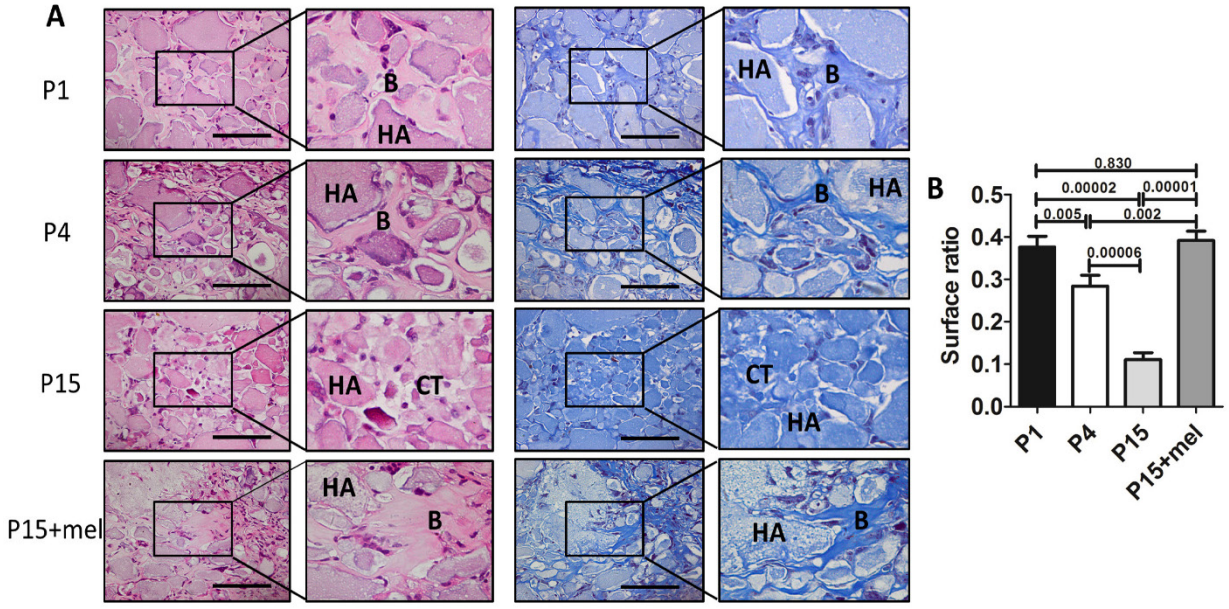

Figure 4. Melatonin treatment improves ectopic osteogenesis of long-term passaged BMMSCs. Rat BMMSC (DMSO-treated P1, P4, P15 BMMSCs and melatonin-treated P15 BMMSCs) cell sheets combined with 20 mg HA/TCP were transplanted subcutaneously into nude mice for 8 weeks. (**A**) New bone formation of BMMSCs was detected by H&E staining and Masson's trichrome staining (n=4) (Abbreviation: B, bone; HA, HA-TCP; CT, connected tissue). Scale bar, 100 μm. (**B**)The surface ratio of new bone formed by BMMSCs in each groups was analyzed by Image-Pro Plus 6.0 (n=4). Data are shown as mean±SD. *P* value is presented in each graph.

To confirm whether the effect of melatonin treatment is conservative between different species, we further investigated the function of melatonin treatment on long-term passaged human mesenchymal stem cells (hBMMSCs). Colony forming, proliferation and osteogenic differentiation assay confirmed that hBMMSCs of 25th passage showed significant function deficiency compared with P1, P4 and P15 hBMMSCs (n=3, p<0.05) (Fig. S2, A to E). In accordance with the results of rat BMMSCs, long-term treatment of melatonin largely prevented stemness loss of P25 hBMMSCs (n=3, p<0.05) (Fig. S2, A to E).

Melatonin preserves the function of long-term passaged BMMSCs in bone repair and bone regeneration.

One of the major applications of BMMSCs cell therapy is bone repair and regeneration. Since melatonin significantly improved the self-renewal and osteogenic differentiation of P15 BMMSCs *in vitro*, we next investigated whether melatonin improves *in vivo* osteogenesis of long-term passaged BMMSCs. Melatonin-treated P15 BMMSCs or DMSO-treated P1, P4, P15 BMMSCs were transplanted subcutaneously into nude mice for 8 weeks. H&E staining and Masson's trichrome staining showed that new bone formation capacity of BMMSCs was gradually decreased after *in vitro* passaging (Fig. 4, A and B). The bone volume formed by P15 BMMSCs was only 28% of that formed by P1 BMMSCs (n=4, p<0.001) (Fig. 4, A and B). Importantly, melatonin treatment increased new bone formation of P15 BMMSCs 3.5-fold compared with DMSO-treated P15 BMMSCs (n=4, p<0.001). Bone volume formed by melatonin-treated P15 BMMSCs was even comparable with that formed by P1 BMMSCs (n=4, p>0.05) (Fig. 4, A and B).

We next confirmed the function of melatonin on BMMSCs-mediated bone repair using a rat calvarial critical defect regeneration model. Melatonin-treated P15 BMMSCs or DMSO-treated P1, P4, P15 BMMSCs combined with HA/TCP were transplanted into critical calvarial defects of rat for 12 weeks. Micro-CT imaging demonstrated that the restorative effect of P1, P4 and P15 BMMSCs on calvarial defect was gradually declined (Fig. 5, A and B). P4 BMMSCs restored 75% of the bone volume formed by P1 BMMSCs (n=4, p<0.05), while P15 BMMSCs only formed 31% of the bone volume of P1 BMMSCs (n=4, p<0.001). Moreover, H&E staining exhibited that P1 or P4 BMMSCs regenerated large amount of new bone from the edge to the center of calvarial defect, while P15 BMMSCs only formed a small amount of new bone at the edge of defect (Fig. 5C). Of note, the skull restoration of melatonin-treated P15 BMMSCs was 3 times of DMSO-treated P15 BMMSCs (n=4, p<0.001) (Fig. 5, A and B). The new bone volume in melatonin-treated P15 BMMSCs group was even greater than that of P4 BMMSCs group (n=4, p<0.05), and equal to that of P1 BMMSCs group (n=4, p>0.05) (Fig. 5A and B). Histological analysis confirmed that melatonin-treated P15 BMMSCs, which formed sufficient new bone from edge to the center of

calvarial defect, functioned identically as P1 BMMSCs on bone regeneration (Fig. 5C).

BMMSCs play central role in bone remodeling and have been recently used for osteoporosis treatment *via* systemic transplantation [50]. Therefore, we further investigated whether melatonin preserves the function of long-term passaged BMMSCs in osteoporosis treatment. We established ovariectomy (OVX)-induced osteoporosis in female rats and transplanted P1, P4, P15 or melatonin-treated P15 BMMSCs *via* tail vein into OVX rats. Ten weeks after BMMSCs therapy, micro-CT analysis confirmed significant bone loss in OVX rats, compared with Sham surgery group (n=6, $p<0.001$). We found that P1 or P4 BMMSCs injection elevated the bone mineral density (BMD) and trabecular bone volume in osteoporosis rats (n=6, $p<0.001$), whereas P15 BMMSCs (n=6, $p>0.05$) failed to prevent bone loss after OVX (Fig. 6, A and B). Notably, melatonin-treated P15 BMMSCs significantly enhanced bone mass and trabecular bone volume of OVX rats by about 30% (n=6, $p<0.01$). The effect of melatonin-treated P15 BMMSCs was comparable with P4 BMMSCs (n=6, $p>0.05$) and slightly lower than P1 BMMSCs (n=6, $p<0.05$) (Fig. 6, A and B). Moreover, H&E staining assay and three-point bending test confirmed the results of micro-CT analysis (Fig. 6, C and D). To investigate the mechanism that melatonin promotes P15 BMMSCs therapy for osteoporosis, we performed calcein labeling analysis and TRAP staining to detect bone formation and bone resorption. Calcein labeling assay exhibited that P1 BMMSCs transplantation potently inhibited the decline of bone formation in trabecular bone after OVX (n=6, $p<0.001$) (Fig. 6E).

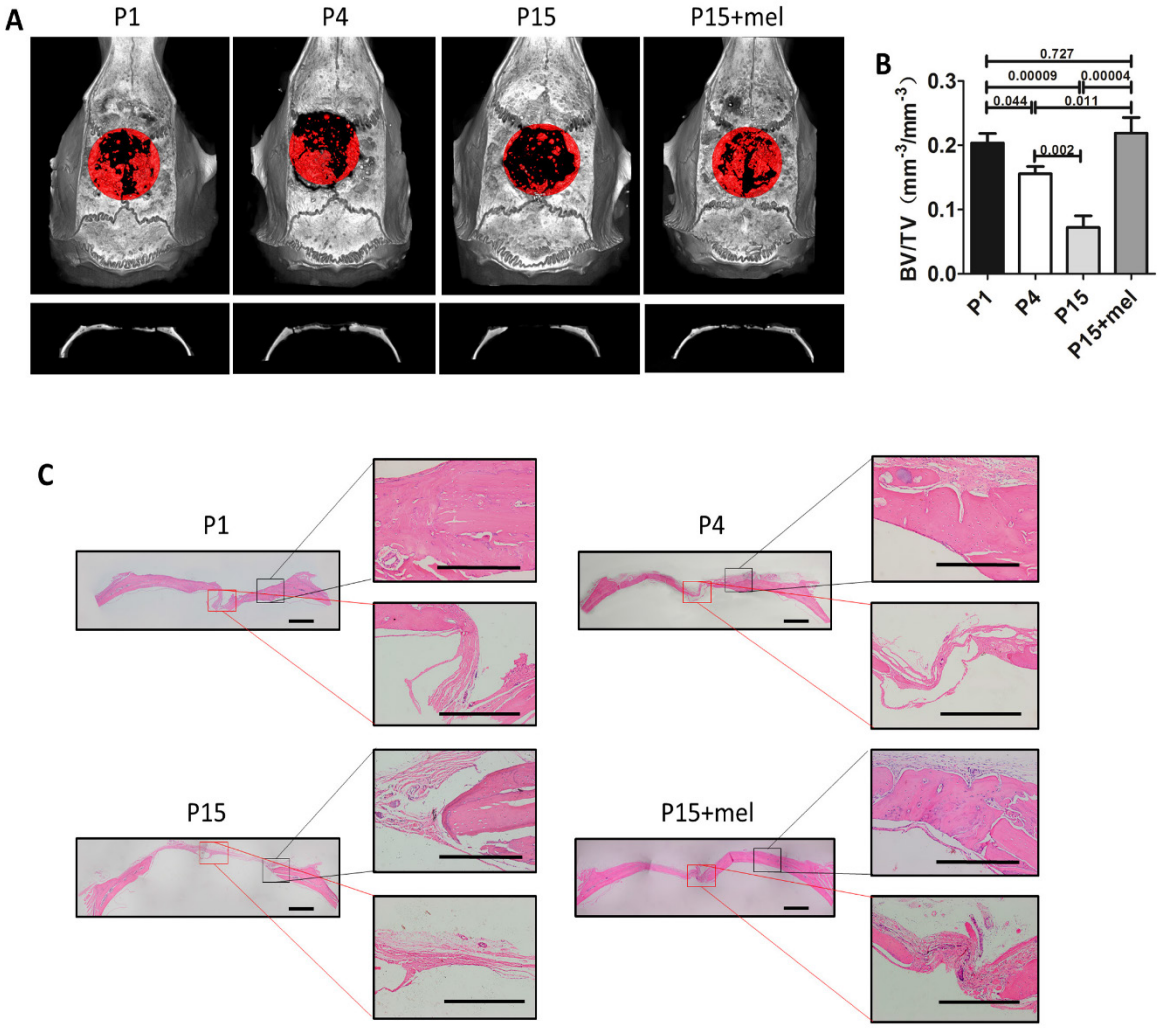

Figure 5. Melatonin treatment improves calvarial defect repair of long-term passaged BMMSCs. Rat BMMSC (DMSO-treated P1, P4, P15 BMMSCs and melatonin-treated P15 BMMSCs) cell sheets composed with 50 mg HA/TCP were transplanted to repair critical size calvarial defects for 12 weeks. (**A**) Calvarial bone newly formed by BMMSCs was detected by micro-CT imaging through vertex and coronal plane. New bone formation was marked by red areas (n=4). (**B**) Bone volume/total volume (BV/TV) of new bone was analyzed by micro-CT (n=4). (**C**) H&E staining was performed to reveal new bone formation from the edge to the center of calvarial defects (n=4). Scale bar of images on the left, 1 mm; Scale bar of images on the right, 500 μm. Data are shown as mean±SD. *P* value is presented in each graph.

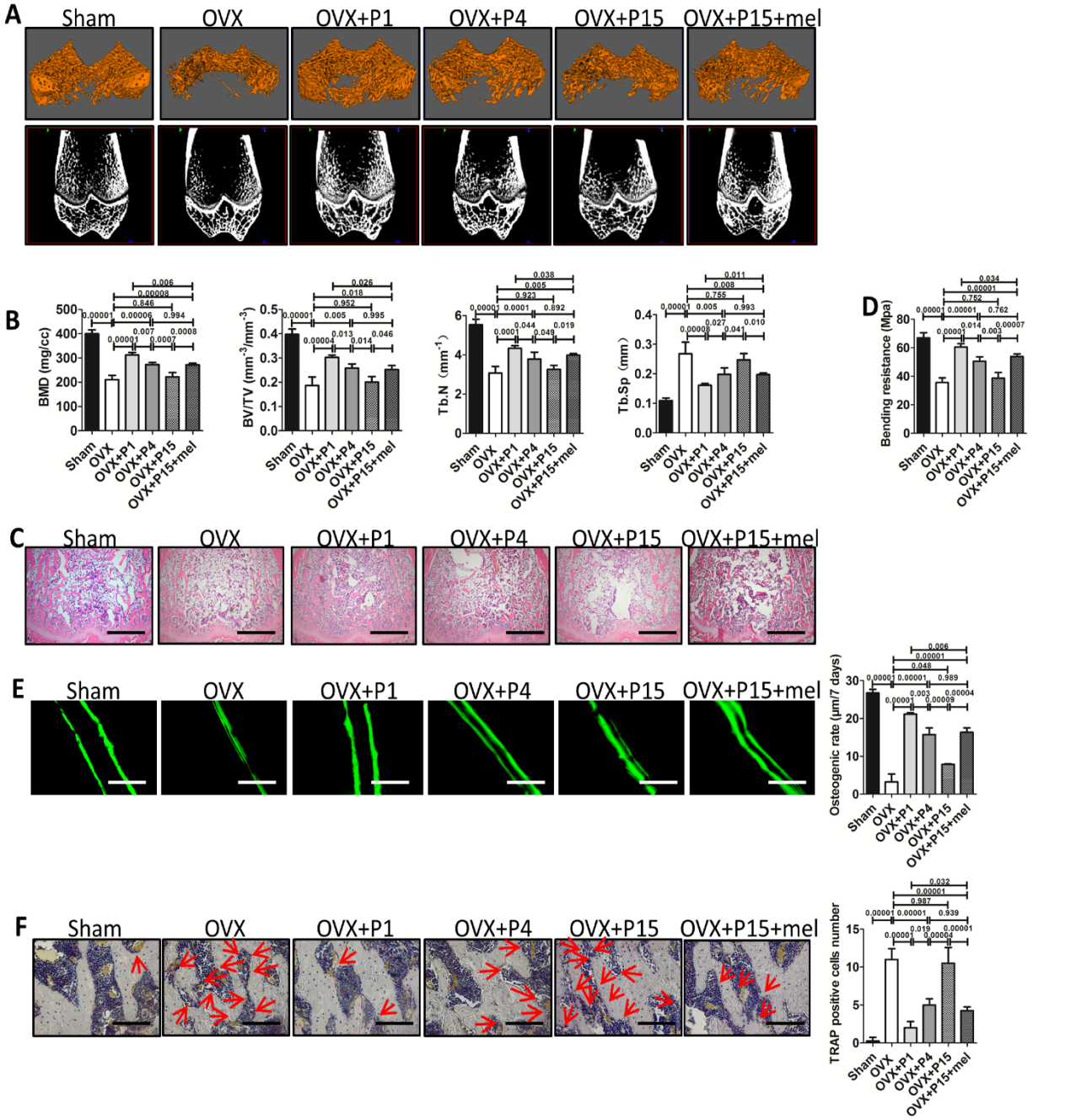

Figure 6. Melatonin treatment improves osteoporosis treatment of long-term passaged BMMSCs. Rat BMMSCs (DMSO-treated P1, P4, P15 BMMSCs and melatonin-treated P15 BMMSCs) were injected subcutaneously into OVX rats for 10 weeks. Sham group and OVX group were treated with equal volume of PBS. (**A**) Trabecular bone of distal parts of the right femurs was detect by micro-CT imaging. Reconstructed 3-dimensional structure and 2-dimensional image of coronal plane were presented (n=6). (**B**) Bone mineral density (BMD), bone volume/total volume (BV/TV), trabecular bone number (Tb.N) and trabecular bone space (Tb.Sp) were analyzed by micro-CT (n=6). (**C**) Trabecular bone structure of distal right femurs was analyzed by H&E staining (n=6). Scale bar, 1 mm. (**D**) Left femurs were used for three-point bending test to evaluate bending resistance (n=6). (**E**) Calcein labeling in distal part of left femurs was observed under fluorescence microscope. Distance between two fluorescent strips was measured with Image pro software (n=6). Scale bar, 100 μm. (**F**) TRAP staining was performed to detect osteoclasts in distal part of right femurs. TRAP+ osteoclasts were marked by red arrows (n=6). Scale bar, 100 μm. Data are shown as mean±SD. *P* value is presented in each graph.

The capacity of P15 BMMSCs to preserve bone formation of OVX rats was decreased by 60% compared with P1 BMMSCs (n=6, $p<0.001$). In accordance, osteogenic rate of rats received melatonin treated-P15 BMMSCs was twice as fast as that of P15 BMMSCs treatment (n=6, $p<0.001$). Melatonin-treated P15 BMMSCs showed similar effect as P4 BMMSCs on promoting bone formation (n=6, $p>0.05$) (Fig. 6E). Moreover, TRAP staining showed that P1 BMMSCs was more potent than P15 BMMSCs to inhibit redundant bone resorption after OVX (Fig. 6F). Melatonin significantly prevented the decline of anti-osteoclastogenesis capacity of BMMSCs after long-term culture (n=6, $p<0.001$) (Fig. 6F).

Melatonin improves immunomodulatory property of long-term passaged BMMSCs in immune therapy.

Immunomodulatory property emerges as an important character of BMMSCs. One hot field of BMMSCs applications is immune therapy [48]. To investigate whether melatonin also preserves the immune-regulation capacity of long-term cultured BMMSCs, we adopted experimental colitis rat model, a widely used animal model of inflammatory colitis. Five days after dextran sulfate sodium (DSS) feeding, rats developed typical symptoms of inflammatory colitis, including loss of weight, diarrhea, bloody stool, and death (Fig. 7, A to C). Histological analysis confirmed that DSS feeding caused severe inflammation and damage in colon mucosa (n=4, p<0.001) (Fig. 7, D and E). As reported, administration of P1 or P4 BMMSCs significantly alleviated DSS-induced body weight loss (Fig. 7B), diarrhea, bloody stool (Fig. 7C), colon inflammation and damage (Fig. 7, D and E), and totally prevented the death of colitis rats (n=4, p<0.001) (Fig. 7A). However, administration of P15 BMMSCs only resulted in modest improvement of colitis (n=4, p>0.05) (Fig. 7, A to E). Importantly, infusion of melatonin-treated P15 BMMSCs was more effective than P15 BMMSCs to elevate survival rate (n=4, p<0.01), inhibit body weight loss, ameliorate symptoms, and improve inflammation and damage in colitis rat (n=4, p<0.05) (Fig. 7, A to E). Moreover, we also assayed the effect of melatonin treatment on human BMMSCs for experimental colitis treatment. In accordance, P25 hBMMSCs failed to cure experimental colitis of rats (n=4, p>0.05), whereas treatment of melatonin partially rescued the therapeutic dysfunction of P25 hBMMSCs (n=4, p<0.05) (Fig. S3, A to E). Taken together, these results indicate that melatonin treatment improves the immune therapy of long-term passaged BMMSCs.

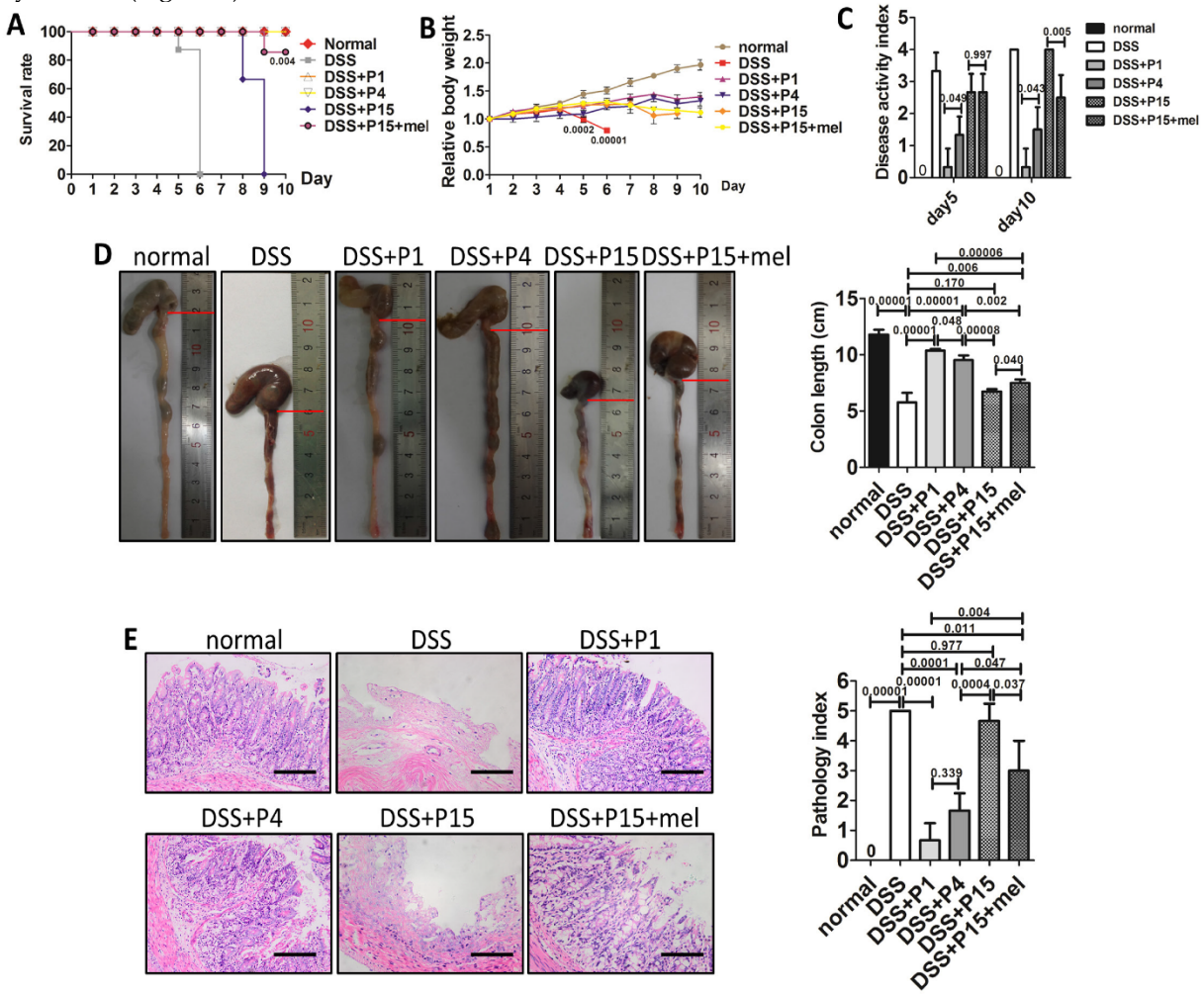

Figure 7. Melatonin treatment improves therapeutic effect of long-term passaged BMMSCs on experimental colitis. Rats were administrated with DMSO-treated P1, P4, P15 rat BMMSCs or melatonin-treated P15 rat BMMSCs *via* tail vein respectively at day 3 of DSS feeding. Normal group and DSS group were injected with equal volume of PBS. (**A**) Survival of rats was recorded every day for 10 days (n=4). (**B**) Body weights were recorded every day for 10 days. The relative change of body weight was calculated (n=4). (**C**) Disease activity index (DAI) was evaluated at day 5 and day 10 according to the symptoms (n=4). (**D**) Colon length was measured at day 10 (n=4). (**E**) H&E staining was performed to detect the histological changes of colon isolated at day 10 (n=4). The pathological index of each colon was calculated (n=4). Scale bar, 100 μm. Data are shown as mean±SD. *P* value is presented in each graph.

Melatonin functions by inhibiting oxidative damage and cell senescence through receptor-independent pathway.

We then explored the mechanism of melatonin to prevent stemness loss of long-term passaged BMMSCs. ROS is a crucial factor induced cellular senescence during *in vitro* expansion [51, 52]. Melatonin is reported to prevent cellular senescence by inhibiting oxidative damage [40]. We found that intracellular ROS levels were gradually increased during BMMSCs passaging (Fig. 8A). The mRNA and protein levels of superoxide dismutase-2 (SOD2), an enzyme efficiently scavenging intracellular ROS, were gradually decreased in P1, P4 and P15 BMMSCs. Accordingly, melatonin treatment decreased ROS levels of P15 BMMSCs by 53% (n=3, $p<0.001$) and increased SOD2 expression 2-fold (n=3, $p<0.001$), compared with DMSO-treated P15 BMMSCs (Fig. 8, A to C, Fig. S4, A and Fig. S5, A).

p53 pathway, which is activated by ROS or telomere shortening during cell replication, inhibits proliferation and self-renewal of SCs [53]. We examined the expression of p53 and its downstream regulator p16. In accordance with ROS accumulation during long-term culture, the expression of p53 and p16 was gradually increased in P1, P4 and P15 BMMSCs (Fig. 8, D and F, Fig. S4, B, Fig. S5, B and C). Melatonin treatment significantly decreased p53 (n=3, $p<0.05$) and p16 (n=3, $p<0.001$) levels in P15 BMMSCs (Fig. 8, D and F, Fig. S4, B, Fig. S5, B and C).

The multipotency of stem cells is controlled by a cluster of master genes [54]. Among them, NANOG is crucial for maintaining self-renewal and undifferentiated state of MSCs [55]. To investigate the mechanism that melatonin improves osteogenic differentiation of passaged BMMSCs, we examined the expression of NANOG by real-time RT-PCR, western blot and immunofluorescence analysis. Both mRNA and protein levels of NANOG were gradually decreased during long-term passaging of BMMSCs (Fig. 8, E and F, Fig. S4, B and Fig. S5, D). Accordingly, melatonin treatment increased NANOG expression in P15 BMMSCs more than 2-fold (n=3, $p<0.001$) to the level comparable with P1 BMMSCs (Fig. 8, E and F, Fig. S4, B and Fig. S5, D). Taken together, the results suggest that melatonin preserves stemness of BMMSCs by inhibiting oxidative stress and p53-pathway, and promoting NANOG expression.

To determine whether melatonin functioned through receptor-dependent or -independent pathway in our study, we used luzindole (LUZ), a non-selective antagonist of melatonin receptors, to inhibit signaling mediated by melatonin receptors. Firstly, real-time RT-PCR and western blot assay showed that either MEL-1A-R (MT1) or MEL-1B-R (MT2) showed no difference between P15 BMMSCs treated with DMSO, melatonin or mel+LUZ (n=3, $p>0.05$) (Fig. 8, G and P, Fig. S4, C). Secondly, luzindole did not affect the effect of melatonin on stemness preservation of long-term passaged BMMSCs (n=3, $p>0.05$) (Fig. 8, H to K). Meanwhile, the expression levels of p53, p16 and Nanog were similar between BMMSCs of P15+mel and P15+mel+LUZ (n=3, $p>0.05$) (Fig. 8, M, N and P, Fig. S4, C). Thirdly, with addition of luzindole, melatonin still reduced ROS level and elevated SOD-2 expression of P15 BMMSCs (n=3, $p<0.01$) (Fig. 8, O and P, Fig. S4, C). Taken together, the results suggested that melatonin function through receptor-independent pathway to preserve stemness of BMMSCs during long-term culture.

Discussion

Loss of stemness during *in vitro* expansion leads to failure of MSCs cell therapy [8-14], which is becoming a crucial issue hindering clinical application of MSCs. In this study, we developed a novel strategy based on specific small molecule to preserve the stemness of BMMSCs. By comparing a number of small molecules with anti-aging and stem cell-preserving properties, we found melatonin was the best to prevent stemness loss of BMMSCs during long-term culture. Treatment of low-dose melatonin largely preserved self-renewal and osteogenic differentiation capacity of long-term cultured rat or human BMMSCs. Importantly, based on ectopic osteogenesis, critical calvarial defect repair and osteoporosis treatment models, we certified that melatonin treatment largely maintained the function of long-term passaged BMMSCs in bone repair and regeneration *in vivo*. Using an experimental colitis model, we further confirmed that melatonin also partly preserved the immune-modulating property of rat or human BMMSCs after long-term culture. Taken together, our study highlights the promising effect of melatonin on BMMSCs protection during long-term *in vitro* passaging.

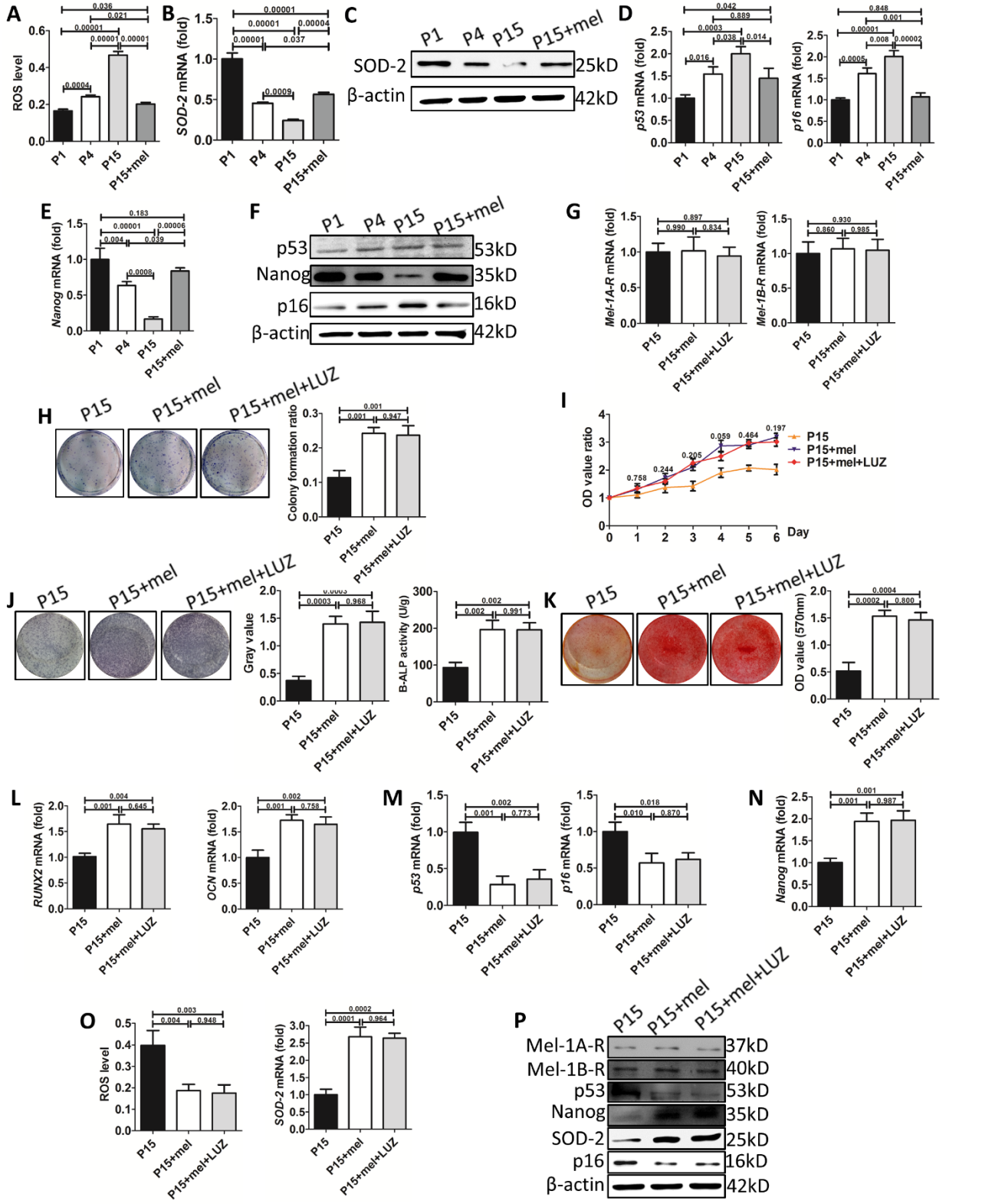

Figure 8. Melatonin treatment decreases ROS levels, inhibits p53 pathway, and preserves NANOG expression in long-term passaged BMMSCs. (A-F) *In vitro* passaged rat BMMSCs of P1, P4, P15 treated with DMSO or 10 nM melatonin were used in following analysis. (A) ROS levels of BMMSCs were measured by flow cytometer (n=3). (B) *Sod2* mRNA levels of BMMSCs were detected by real-time RT-PCR. *β-actin* was used as the loading control for quantification (n=3). (C) Expression of SOD2 protein was detected by western blot analysis. β-actin was used as the loading control (n=3). (D and E) Real-time RT-PCR was performed to measure *p53*, *p16* (D) and *Nanog* (E) mRNA levels in BMMSCs (n=3). (F) Expression of p53, p16 and NANOG protein was detected by western blotting (n=3). (G-P) BMMSCs were treated with DMSO, melatonin or melatonin plus LUZ from the 1st passage to the 15th passage. (G) *Mel-1A-R* and *Mel-1B-R* mRNA levels in BMMSCs were analysis by realtime RT-PCR. (n=3). (H) CFU-F formation of BMMSCs was detected by toluidine blue staining and calculated (n=3). (I) Proliferation of BMMSCs was detected from day 0 to day 6 (n=3). (J) ALP staining and ELISA analysis were performed to detect the activity of ALP of BMMSCs after 7-day osteogenic induction (n=3). (K) Mineralized nodules formed by BMMSCs were tested by alizarin red staining after 28-day osteogenic induction and quantified (n=3). (L-N) *Runx2*, *Ocn* (L), *p53*, *p16* (M) and *Nanog* (N) mRNA levels in BMMSCs were analyzed by Realtime RT-PCR (n=3). (O) ROS levels and *Sod2* mRNA levels in BMMSCs (n=3). (P) Expression of Mel-1A-R, Mel-1B-R, SOD2, p53, p16 and NANOG protein was detected by western blot analysis. (n=3). Data are shown as mean±SD. *P* value is presented in each graph.

Our study provided a novel strategy to prevent the loss of stemness of BMMSCs during long-term passaging. We cultured BMMSCs with low concentration of melatonin since the beginning of *in vitro* passaging to avoid the potential side effect of high-dose melatonin treatment. *In vitro* and *in vivo* data confirmed that long-term cultured BMMSCs treated with melatonin showed comparable therapeutic effects on osteogenesis, bone remodeling regulation and immune modulation, suggesting the stemness of BMMSCs was largely preserved by melatonin. Furthermore, compared with previous methods reported to improve *in vitro* stem cells expansion [17-25], our strategy has a number of advantages. (I) High efficiency: our results showed that P15 BMMSCs treated with melatonin preserved over 85% of the self-renewal and osteogenic differentiation capacity of P1 BMMSCs *in vitro*, and exhibited nearly equal therapeutic function as P1 BMMSCs in bone regeneration and repair *in vivo*. Furthermore, melatonin treatment also partly improved the immunomodulatory property of P15 BMMSCs. (II) Specificity: we found that 10 nM melatonin functioned in long-term passaged BMMSCs but not in short-term passaged BMMSCs, suggesting melatonin specifically prevents the stemness loss during long-term passaging. (III) Safety: melatonin is a natural small molecule secreted by pineal and several tissues in animals and human beings. Thorough animal and clinic studies have confirmed the low toxicity of melatonin treatment at a range of low-dose [56, 57]. Rats can even endure treatment of 200 mg/kg melatonin [56]. (IV) Convenience: in our strategy, only one small molecule was supplemented into conventional culture medium. It is very practical to be applied in large-scale commercial production of stem cells. With these advantages, low concentration melatonin treatment would be a practical and efficient strategy to improve cell therapy of *in vitro* expanded BMMSCs.

Previous studies have shown that melatonin treatment improves MSCs cell therapy for various diseases. Lee and colleagues showed that melatonin treatment improves the mobility of umbilical cord blood-derived MSCs to improve skin wound healing [44]. Three research groups reported that melatonin treatment improves adipose-derived MSCs therapy for acute lung ischemia-reperfusion injury [43], sepsis-induced kidney injury [42], and acute interstitial cystitis [58]. Melatonin treatment has also been applied in osteoporosis treatment partly by promoting osteogenic differentiation of BMMSCs [39, 59]. In these studies, the application of melatonin aimed to promote the function of MSCs and focused on the effect of melatonin on normal MSCs [37, 38, 40-44, 60]. However, in our study, we found low-concentration melatonin functioned as a protector but not as a regulator for BMMSCs. Low-dose melatonin treatment did not affect the function of BMMSCs at early passage, whereas efficiently prevented the loss of stemness of BMMSCs during long-term in vitro expansion. The notion that melatonin functions as a protector was supported by recent studies [45, 61]. It might explain the question why melatonin treatment improves MSCs cell therapy for various diseases. Therefore, our study proposed novel application of melatonin in stem cell expansion and therapy. Further investigations are needed to explore whether melatonin plays a protector role to improve MSCs cell therapy in all aforementioned disease models.

The stemness loss and dysfunction of stem cells during long-term passaging may credit to cell senescence. Therefore, four natural small molecule compounds were selected from the compound library in consideration of their pharmacologic action on cellular senescence or aging. Rapamycin, which is closely related with nutrient availability and energy supplies [62], has been confirmed to delay senescence or extend lifespan in mammals through inhibition of mTOR signaling [31, 62]. Resveratrol is also reported as a promising molecule for lifespan extension in multiple model organisms, health promotion and disease amelioration in mammals through activation of SIRT1 signaling [63]. In addition, resveratrol also delays cell replicative senescence and promotes the osteogenesis of MSCs [64, 65]. Quercetin is a well-known ROS scavenger and a regulator of stem cell function [66, 67]. Melatonin is generally accepted as a compound with great potential of ROS elimination [38] and intracellular signaling regulation [68]. Its biological effects of senescence delaying, ossification promotion and immune regulation have been validated in *in vitro* and *in vivo* studies [69-72]. Unexpectedly, these small molecules played distinct function on long-term passaged BMMSCs. Melatonin performed much better than rapamycin, resveratrol or quercetin to preserve the stemness of long-term passaged BMMSCs. The inconsistent function of anti-aging small molecules suggested distinct mechanism between age-related cellular senescence *in vivo* and replicative cellular senescence *in vitro*. This notion was supported by the study of Fickert and colleagues [7], who showed that the reduction of osteogenic differentiation capacity of long-term cultured human MSCs is not age-dependent. Furthermore, stem cells will lose their identity and function when isolated from physiological micro-environment [16]. The dysfunction of long-term passaged BMMSCs might not only due to replicative

senescence but also due to disturbance of extracellular signaling. It is interesting to compare the signaling pathways regulated by the four small molecules and find out the molecular basis of the advantage of melatonin.

Melatonin regulates BMMSCs through various pathways [40, 73]. On the one hand, melatonin directly regulates BMMSCs differentiation by modulating signaling transduction through MT1 or MT2 receptor [40]. The activation of MLT receptor by melatonin can promote the expression of master transcriptional factors such as Runx2 and Osterix, and activate signaling pathways such as Wnt pathway. On the other hand, melatonin regulates BMMSCs function through affecting microenvironment. Melatonin is commonly known as a powerful redox regulator and cellular protective factor to protect BMMSCs from cellular damage through receptor-independent manner [38, 40, 74]. In our study, we found that luzindole, a non-selective antagonist of melatonin receptors, failed in blocking melatonin function on P15 BMMSCs. These data suggested that low-dose melatonin treatment did not function directly via melatonin receptors on BMMSCs. Of note, with addition of luzindole, melatonin still reduced ROS levels and elevated SOD-2 expression of P15 BMMSCs. ROS, which causes damage of DNA, protein and lipids, is a key factor triggering cellular damage and senescence. It is reported that excessive oxidative stress inhibits osteogenic differentiation and self-renew of BMMSCs, whereas antioxidative treatment could alleviate the function loss of aged BMMSCs [75]. Therefore, our results indicated that low-dose melatonin majorly functions *via* receptor-independent pathway (anti-oxidation) to modulate ROS in the microenvironment of BMMSCs,

The mechanism of stem cell senescence during in vitro culture is widely investigated. Oxidative damage is considered to be a key mechanism of cell senescence and stem cell dysfunction during aging. Excessive oxidative stress increases expression of p53 and p16, which triggers signaling pathway of cell apoptosis and senescence. Oxidative stress could also directly or indirectly inhibit transcription factors controlling the stemness. Numbers of studies reported that low oxygen tension improves in vitro expansion of stem cell, indicating that ROS accumulation induces stem cell senescence and dysfunction during in vitro culture. In this study, we found that the stemness and function of BMMSCs were decreased after long-term passaged, which is in accordance with the accumulation of ROS. Accordingly, the expression of p53 and p16, two important downstream molecules of ROS, was also significantly increased in long-term cultured BMMSCs. Moreover, functional analysis confirmed that melatonin improved BMMSCs stemness majorly by direct scavenging excessive ROS, but not by activating melatonin receptor-mediated signaling pathways. Taken together, our results indicated that melatonin decreased oxidative damage in long-term cultured BMMSCs to prevent the activation of p53 and p16 pathways, resulting in improved stemness and function of BMMSCs.

Our results showed that melatonin treatment enhanced the expression of ALP, OCN and Runx2 in long-term passaged BMMSCs. However, treatment of melatonin showed little influence on these genes expression in early-passage BMMSCs. Considering that melatonin was only supplied to basal medium during long-term passaging, but not to conditioned medium during osteogenic induction, it is highly possible that melatonin functioned by preventing the decrease of osteogenic differentiation capacity of BMMSCs during long-term passaging, but not directly promoting their differentiation. Our data suggested that melatonin preserved ALP, OCN and Runx2 in long-term passaged BMMSCs through receptor-independent pathway further supported the notion.

To verify whether our strategy improves cell therapy of long-term passaged BMMSCs, we selected ectopic bone formation model, calvarial defect model, OVX-induced osteoporosis model and experimental colitis model, representing the major applications of BMMSCs in clinic. Among them, ectopic bone formation model and calvarial defect model were adopted to verify bone regeneration and repair properties of BMMSCs; Osteoporosis model was used to certify the physiological capacity of BMMSCs to regulate bone-remodeling balance; Experimental colitis model was applied to examine the immunoregulatory property of BMMSCs. Of note, our data exhibited that melatonin treatment significantly improved therapeutic effect of long-term passaged BMMSCs on all models. To our knowledge, it is the first strategy that simultaneously improves BMMSCs cell therapy for osteogenesis, bone remodeling regulation and immune modulation. Since all fields of BMMSCs cell therapy face shortage of cell sources, our strategy possesses a wild aspect of application in the future.

Conclusion

In current study, we set out to establish a small molecule-based strategy to improve cell therapy of long-term cultured BMMSCs. By comparing small molecules with anti-aging and SCs preservation properties, we found that melatonin efficiently prevented the stemness loss of rat BMMSCs during

long-term *in vitro* culture. Moreover, heterotopic osteogenesis assay, skull maximum defect repair assay, osteoporosis treatment and experimental colitis therapy assay strongly certified that melatonin preserved the therapeutic effect of long-term passaged BMMSCs on bone regeneration and immunotherapy *in vivo*. Mechanistically, melatonin functioned by activating antioxidant defense system, inhibiting the pathway of cell senescence, and preserving the expression of gene governing the stemness through receptor-independent pathway. Taken together, our findings indicate that melatonin treatment is an efficient and practical strategy to improve *in vitro* expansion of BMMSCs for tissue engineering and cytotherapy.

Supplementary Material

Supplementary tables and figures.
http://www.thno.org/v06p1899s1.pdf

Abbreviations

ALP: alkaline phosphatase; B-ALP: bone alkaline phosphatase; α-MEM: minimum essential medium α; BMMSCs: bone marrow mesenchymal stem cells; BMD: bone mineral density; BV/TV: bone volume/total volume; CCK-8: cell counting kit-8; CFU-F: fibroblastic Colony-forming unit; DAI: disease activity index; DCFH-DA: 2', 7'-dichlorofluorescein diacetate; DMSO: dimethyl sulfoxide; DSS: dextran sulfate sodium; ECM: extracellular matrix; EDTA: ethylene diamine tetraacetic acid; EGF: epidermal growth factor; ESCs: embryonic stem cells; FGF2: fibroblast growth factor 2; FGF4: fibroblast growth factor 4; HA-TCP: hydroxyapatite/tricalcium phosphate; H&E: hematoxylin and eosin; iPSCs: induced pluripotent stem cells; Klf4: kruppel like factor 4; MSCs: mesenchymal stem cells; mTORC1: mammalian target of rapamycin complex 1; OCN: osteocalcin; OCT4: octamer-binding transcription factor 4; OVX: ovariectomy; P1: 1st passage; P4: 4th passage; P15: 15th passage; p53: tumor protein 53; p16: tumor protein 16; PBS: phosphate buffered saline; PDGF: platelet derived growth factor; ROS: reactive oxygen species; RUNX2: runt-related transcription factor 2; SCs: stem cells; Sirt1: sirtuin1; SOD2: superoxide dismutase 2; Tb.N: trabecular bone number; Tb.Sp: trabecular bone space; TRAP: tartrate-resistant acid phosphatase; LUZ: luzindole; HPLC: high performance liquid chromatography.

Acknowledgments

We thank Hua Ni, Leiguo Ming, Xiaolin Xu and Jiangtao Guan for technical assistance of cytology and animal experiment in Research and Development Center for Tissue Engineering, Fourth Military Medical University, Xi'an, Shaanxi, China.

Funding

This work was supported by grants from the Nature Science Foundation of China (81470710, 81470679, 31030033) and the National Major Scientific Research Program of China (2011CB964700).

Author contributions

Yan Jin, Zhihong Deng, Yi Shuai and Li Liao conceived and designed the study. Yan Jin and Zhihong Deng supervised the project. Yi Shuai and Li Liao performed the experiments, analyzed the data, and wrote the manuscript. Yan Jin and Zhihong Deng reviewed the manuscript. Xiaoxia Su, Yang Yu, Bingyi Shao, Huan Jing and Xinjing Zhang participated in the sample collection of partial animal experiments.

Competing Interests

The authors declare that they have no competing interests.

References

1. Parekkadan B, Milwid JM. Mesenchymal stem cells as therapeutics. Annual review of biomedical engineering. 2010; 12: 87-117.
2. Caplan AI, Correa D. The MSC: an injury drugstore. Cell Stem Cell. 2011; 9: 11-5.
3. [Internet] National Institutes of Health.. A service of the U.S. https://www.clinicaltrials.gov/.
4. Baker N, Boyette LB, Tuan RS. Characterization of bone marrow-derived mesenchymal stem cells in aging. Bone. 2015; 70: 37-47.
5. Kim J, Kang JW, Park JH, Choi Y, Choi KS, Park KD, et al. Biological characterization of long-term cultured human mesenchymal stem cells. Arch Pharm Res. 2009; 32: 117-26.
6. Wagner W, Bork S, Lepperdinger G, Joussen S, Ma N, Strunk D, et al. How to track cellular aging of mesenchymal stromal cells? Aging (Albany NY). 2010; 2: 224-30.
7. Fickert S, Schroter-Bobsin U, Gross AF, Hempel U, Wojciechowski C, Rentsch C, et al. Human mesenchymal stem cell proliferation and osteogenic differentiation during long-term ex vivo cultivation is not age dependent. J Bone Miner Metab. 2011; 29: 224-35.
8. Furlani D, Li W, Pittermann E, Klopsch C, Wang L, Knopp A, et al. A transformed cell population derived from cultured mesenchymal stem cells has no functional effect after transplantation into the injured heart. Cell transplantation. 2009; 18: 319-31.
9. Crisostomo PR, Wang M, Wairiuko GM, Morrell ED, Terrell AM, Seshadri P, et al. High passage number of stem cells adversely affects stem cell activation and myocardial protection. Shock. 2006; 26: 575-80.
10. Bustos ML, Huleihel L, Kapetanaki MG, Lino-Cardenas CL, Mroz L, Ellis BM, et al. Aging mesenchymal stem cells fail to protect because of impaired migration and antiinflammatory response. American journal of respiratory and critical care medicine. 2014; 189: 787-98.
11. Choi MR, Kim HY, Park JY, Lee TY, Baik CS, Chai YG, et al. Selection of optimal passage of bone marrow-derived mesenchymal stem cells for stem cell therapy in patients with amyotrophic lateral sclerosis. Neuroscience letters. 2010; 472: 94-8.
12. Castorina A, Szychlinska MA, Marzagalli R, Musumeci G. Mesenchymal stem cells-based therapy as a potential treatment in neurodegenerative disorders: is the escape from senescence an answer? Neural regeneration research. 2015; 10: 850-8.
13. von Bahr L, Sundberg B, Lonnies L, Sander B, Karbach H, Hagglund H, et al. Long-term complications, immunologic effects, and role of passage for outcome in mesenchymal stromal cell therapy. Biology of blood and marrow transplantation : journal of the American Society for Blood and Marrow Transplantation. 2012; 18: 557-64.
14. Sepulveda JC, Tome M, Fernandez ME, Delgado M, Campisi J, Bernad A, et al. Cell senescence abrogates the therapeutic potential of human mesenchymal stem cells in the lethal endotoxemia model. Stem cells. 2014; 32: 1865-77.
15. Farrell MJ, Fisher MB, Huang AH, Shin JI, Farrell KM, Mauck RL. Functional properties of bone marrow-derived MSC-based engineered cartilage are unstable with very long-term in vitro culture. J Biomech. 2014; 47: 2173-82.

16. Jones DL, Wagers AJ. No place like home: anatomy and function of the stem cell niche. Nat Rev Mol Cell Biol. 2008; 9: 11-21.
17. Danet GH, Pan Y, Luongo JL, Bonnet DA, Simon MC. Expansion of human SCID-repopulating cells under hypoxic conditions. J Clin Invest. 2003; 112: 126-35.
18. Estrada JC, Albo C, Benguria A, Dopazo A, Lopez-Romero P, Carrera-Quintanar L, et al. Culture of human mesenchymal stem cells at low oxygen tension improves growth and genetic stability by activating glycolysis. Cell Death Differ. 2012; 19: 743-55.
19. Fehrer C, Brunauer R, Laschober G, Unterluggauer H, Reitinger S, Kloss F, et al. Reduced oxygen tension attenuates differentiation capacity of human mesenchymal stem cells and prolongs their lifespan. Aging Cell. 2007; 6: 745-57.
20. Lin H, Yang G, Tan J, Tuan RS. Influence of decellularized matrix derived from human mesenchymal stem cells on their proliferation, migration and multi-lineage differentiation potential. Biomaterials. 2012; 33: 4480-9.
21. Sun Y, Li W, Lu Z, Chen R, Ling J, Ran Q, et al. Rescuing replication and osteogenesis of aged mesenchymal stem cells by exposure to a young extracellular matrix. FASEB J. 2011; 25: 1474-85.
22. Coutu DL, Francois M, Galipeau J. Inhibition of cellular senescence by developmentally regulated FGF receptors in mesenchymal stem cells. Blood. 2011; 117: 6801-12.
23. Eom YW, Oh JE, Lee JI, Baik SK, Rhee KJ, Shin HC, et al. The role of growth factors in maintenance of stemness in bone marrow-derived mesenchymal stem cells. Biochemical and biophysical research communications. 2014; 445: 16-22.
24. Park IH, Zhao R, West JA, Yabuuchi A, Huo H, Ince TA, et al. Reprogramming of human somatic cells to pluripotency with defined factors. Nature. 2008; 451: 141-6.
25. Tang H, Xiang Y, Jiang X, Ke Y, Xiao Z, Guo Y, et al. Dual expression of hTERT and VEGF prolongs life span and enhances angiogenic ability of aged BMSCs. Biochem Biophys Res Commun. 2013; 440: 502-8.
26. Eliasson P, Rehn M, Hammar P, Larsson P, Sirenko O, Flippin LA, et al. Hypoxia mediates low cell-cycle activity and increases the proportion of long-term-reconstituting hematopoietic stem cells during in vitro culture. Experimental hematology. 2010; 38: 301-10 e2.
27. Guitart AV, Hammoud M, Dello Sbarba P, Ivanovic Z, Praloran V. Slow-cycling/quiescence balance of hematopoietic stem cells is related to physiological gradient of oxygen. Exp Hematol. 2010; 38: 847-51.
28. Chen FM, Shelton RM, Jin Y, Chapple IL. Localized delivery of growth factors for periodontal tissue regeneration: role, strategies, and perspectives. Med Res Rev. 2009; 29: 472-513.
29. Fazel SS, Angoulvant D, Butany J, Weisel RD, Li RK. Mesenchymal stem cells engineered to overexpress stem cell factor improve cardiac function but have malignant potential. J Thorac Cardiovasc Surg. 2008; 136: 1388-9.
30. Li J, Kim SG, Blenis J. Rapamycin: one drug, many effects. Cell Metab. 2014; 19: 373-9.
31. Harrison DE, Strong R, Sharp ZD, Nelson JF, Astle CM, Flurkey K, et al. Rapamycin fed late in life extends lifespan in genetically heterogeneous mice. Nature. 2009; 460: 392-5.
32. Pearson KJ, Baur JA, Lewis KN, Peshkin L, Price NL, Labinskyy N, et al. Resveratrol delays age-related deterioration and mimics transcriptional aspects of dietary restriction without extending life span. Cell metabolism. 2008; 8: 157-68.
33. Lairson LL, Lyssiotis CA, Zhu S, Schultz PG. Small molecule-based approaches to adult stem cell therapies. Annual review of pharmacology and toxicology. 2013; 53: 107-25.
34. Acuna-Castroviejo D, Escames G, Venegas C, Diaz-Casado ME, Lima-Cabello E, Lopez LC, et al. Extrapineal melatonin: sources, regulation, and potential functions. Cellular and molecular life sciences : CMLS. 2014; 71: 2997-3025.
35. Reiter RJ. Pineal melatonin: cell biology of its synthesis and of its physiological interactions. Endocrine reviews. 1991; 12: 151-80.
36. Reiter RJ, Tan DX, Galano A. Melatonin: exceeding expectations. Physiology. 2014; 29: 325-33.
37. Singh M, Jadhav HR. Melatonin: functions and ligands. Drug Discov Today. 2014; 19: 1410-8.
38. Zhang HM, Zhang Y. Melatonin: a well-documented antioxidant with conditional pro-oxidant actions. Journal of pineal research. 2014; 57: 131-46.
39. Amstrup AK, Sikjaer T, Mosekilde L, Rejnmark L. Melatonin and the skeleton. Osteoporosis international : a journal established as result of cooperation between the European Foundation for Osteoporosis and the National Osteoporosis Foundation of the USA. 2013; 24: 2919-27.
40. Luchetti F, Canonico B, Bartolini D, Arcangeletti M, Ciffolilli S, Murdolo G, et al. Melatonin regulates mesenchymal stem cell differentiation: a review. Journal of pineal research. 2014; 56: 382-97.
41. Clafshenkel WP, Rutkowski JL, Palchesko RN, Romeo JD, McGowan KA, Gawalt ES, et al. A novel calcium aluminate-melatonin scaffold enhances bone regeneration within a calvarial defect. Journal of pineal research. 2012; 53: 206-18.
42. Chen HH, Lin KC, Wallace CG, Chen YT, Yang CC, Leu S, et al. Additional benefit of combined therapy with melatonin and apoptotic adipose-derived mesenchymal stem cell against sepsis-induced kidney injury. Journal of pineal research. 2014; 57: 16-32.
43. Yip HK, Chang YC, Wallace CG, Chang LT, Tsai TH, Chen YL, et al. Melatonin treatment improves adipose-derived mesenchymal stem cell therapy for acute lung ischemia-reperfusion injury. Journal of pineal research. 2013; 54: 207-21.
44. Lee SJ, Jung YH, Oh SY, Yun SP, Han HJ. Melatonin enhances the human mesenchymal stem cells motility via melatonin receptor 2 coupling with Galphaq in skin wound healing. Journal of pineal research. 2014; 57: 393-407.
45. Zhou L, Chen X, Liu T, Gong Y, Chen S, Pan G, et al. Melatonin reverses H2 O2 -induced premature senescence in mesenchymal stem cells via the SIRT1-dependent pathway. Journal of pineal research. 2015; 59: 190-205.
46. Ogata Y, Mabuchi Y, Yoshida M, Suto EG, Suzuki N, Muneta T, et al. Purified Human Synovium Mesenchymal Stem Cells as a Good Resource for Cartilage Regeneration. PLoS One. 2015; 10: e0129096.
47. Naito Y, Takagi T, Kuroda M, Katada K, Ichikawa H, Kokura S, et al. An orally active matrix metalloproteinase inhibitor, ONO-4817, reduces dextran sulfate sodium-induced colitis in mice. Inflammation research : official journal of the European Histamine Research Society [et al]. 2004; 53: 462-8.
48. Akiyama K, Chen C, Wang D, Xu X, Qu C, Yamaza T, et al. Mesenchymal-stem-cell-induced immunoregulation involves FAS-ligand-/FAS-mediated T cell apoptosis. Cell Stem Cell. 2012; 10: 544-55.
49. Guo W, He Y, Zhang X, Lu W, Wang C, Yu H, et al. The use of dentin matrix scaffold and dental follicle cells for dentin regeneration. Biomaterials. 2009; 30: 6708-23.
50. Liu Y, Wang L, Liu S, Liu D, Chen C, Xu X, et al. Transplantation of SHED prevents bone loss in the early phase of ovariectomy-induced osteoporosis. J Dent Res. 2014; 93: 1124-32.
51. Busuttil RA, Rubio M, Dolle ME, Campisi J, Vijg J. Oxygen accelerates the accumulation of mutations during the senescence and immortalization of murine cells in culture. Aging Cell. 2003; 2: 287-94.
52. Parrinello S, Samper E, Krtolica A, Goldstein J, Melov S, Campisi J. Oxygen sensitivity severely limits the replicative lifespan of murine fibroblasts. Nat Cell Biol. 2003; 5: 741-7.
53. Bonizzi G, Cicalese A, Insinga A, Pelicci PG. The emerging role of p53 in stem cells. Trends Mol Med. 2012; 18: 6-12.
54. Silva J, Smith A. Capturing pluripotency. Cell. 2008; 132: 532-6.
55. Tsai CC, Su PF, Huang YF, Yew TL, Hung SC. Oct4 and Nanog directly regulate Dnmt1 to maintain self-renewal and undifferentiated state in mesenchymal stem cells. Molecular cell. 2012; 47: 169-82.
56. Jahnke G, Marr M, Myers C, Wilson R, Travlos G, Price C. Maternal and developmental toxicity evaluation of melatonin administered orally to pregnant Sprague-Dawley rats. Toxicological sciences : an official journal of the Society of Toxicology. 1999; 50: 271-9.
57. Sanchez-Barcelo EJ, Mediavilla MD, Tan DX, Reiter RJ. Clinical uses of melatonin: evaluation of human trials. Current medicinal chemistry. 2010; 17: 2070-95.
58. Chen YT, Chiang HJ, Chen CH, Sung PH, Lee FY, Tsai TH, et al. Melatonin treatment further improves adipose-derived mesenchymal stem cell therapy for acute interstitial cystitis in rat. Journal of pineal research. 2014; 57: 248-61.
59. Zhang L, Su P, Xu C, Chen C, Liang A, Du K, et al. Melatonin inhibits adipogenesis and enhances osteogenesis of human mesenchymal stem cells by suppressing PPARgamma expression and enhancing Runx2 expression. Journal of pineal research. 2010; 49: 364-72.
60. Tang Y, Cai B, Yuan F, He X, Lin X, Wang J, et al. Melatonin pretreatment improves the survival and function of transplanted mesenchymal stem cells after focal cerebral ischemia. Cell Transplant. 2013.
61. Liu X, Gong Y, Xiong K, Ye Y, Xiong Y, Zhuang Z, et al. Melatonin mediates protective effects on inflammatory response induced by interleukin-1 beta in human mesenchymal stem cells. Journal of pineal research. 2013; 55: 14-25.
62. Ehninger D, Neff F, Xie K. Longevity, aging and rapamycin. Cell Mol Life Sci. 2014; 71: 4325-46.
63. Bhullar KS, Hubbard BP. Lifespan and healthspan extension by resveratrol. Biochim Biophys Acta. 2015; 1852: 1209-18.
64. Mikula-Pietrasik J, Kuczmarska A, Rubis B, Filas V, Murias M, Zielinski P, et al. Resveratrol delays replicative senescence of human mesothelial cells via mobilization of antioxidative and DNA repair mechanisms. Free Radic Biol Med. 2012; 52: 2234-45.
65. Tseng PC, Hou SM, Chen RJ, Peng HW, Hsieh CF, Kuo ML, et al. Resveratrol promotes osteogenesis of human mesenchymal stem cells by upregulating RUNX2 gene expression via the SIRT1/FOXO3A axis. J Bone Miner Res. 2011; 26: 2552-63.
66. Ishisaka A, Ichikawa S, Sakakibara H, Piskula MK, Nakamura T, Kato Y, et al. Accumulation of orally administered quercetin in brain tissue and its antioxidative effects in rats. Free Radic Biol Med. 2011; 51: 1329-36.
67. Zhou C, Lin Y. Osteogenic differentiation of adipose-derived stem cells promoted by quercetin. Cell Prolif. 2014; 47: 124-32.
68. Luchetti F, Canonico B, Betti M, Arcangeletti M, Pilolli F, Piroddi M, et al. Melatonin signaling and cell protection function. FASEB J. 2010; 24: 3603-24.
69. Koyama H, Nakade O, Takada Y, Kaku T, Lau KH. Melatonin at pharmacologic doses increases bone mass by suppressing resorption through down-regulation of the RANKL-mediated osteoclast formation and activation. J Bone Miner Res. 2002; 17: 1219-29.
70. Son JH, Cho YC, Sung IY, Kim IR, Park BS, Kim YD. Melatonin promotes osteoblast differentiation and mineralization of MC3T3-E1 cells under hypoxic conditions through activation of PKD/p38 pathways. Journal of pineal research. 2014; 57: 385-92.

71. Cardinali DP, Esquifino AI, Srinivasan V, Pandi-Perumal SR. Melatonin and the immune system in aging. Neuroimmunomodulation. 2008; 15: 272-8.
72. Espino J, Pariente JA, Rodriguez AB. Oxidative stress and immunosenescence: therapeutic effects of melatonin. Oxid Med Cell Longev. 2012; 2012: 670294.
73. Maria S, Witt-Enderby PA. Melatonin effects on bone: potential use for the prevention and treatment for osteopenia, osteoporosis, and periodontal disease and for use in bone-grafting procedures. Journal of pineal research. 2014; 56: 115-25.
74. Manchester LC, Coto-Montes A, Boga JA, Andersen LP, Zhou Z, Galano A, et al. Melatonin: an ancient molecule that makes oxygen metabolically tolerable. Journal of pineal research. 2015.
75. Finkel T, Holbrook NJ. Oxidants, oxidative stress and the biology of ageing. Nature. 2000; 408: 239-47.